Synthesis and Applications of Functionalized Pyridinyl Imine Complexes of Palladium

by

Jezreel Cloete

A dissertation submitted in fulfilment of the requirements

For the degree of Master of Science in the Department of Chemistry,

University of the Western Cape

SUPERVISOR: Prof. S.F. Mapolie (University of the Western Cape, Cape Town, SA)

2004

DECLARATION

I declare that **"SYNTHESIS AND APPLICATIONS OF FUNCTIONALIZED PYRIDINYL IMINE COMPLEXES OF PALLADIUM"** is my own work and that all sources I have used or quoted have been indicated and acknowledged by means of references.

……..……

Jezreel Cloete

ACKNOWLEDGEMENTS

I would like to extend my gratitude to the following:

God Almighty through whom all things are made possible

My supervisor, Prof. S.F. Mapolie, for his constant guidance, support and patience and developing my skills in the field of research.

The National Research Foundation for financial assistance.

The University of the Western Cape technical staff, Mr. T. Lesch, Mr. A. Mantyi and Mr. B. De Wet.

My colleagues in our department and friends, Ms S. Botha, Mr. G. Smith, Mrs D. Dooling-Mopp, Ms N. Maithufi, Ms F. Zigxashi, and especially Ms L.V. Wyatt.

My family, especially my mother and father for their continuous support, encouragement and guidance throughout my studies.

ABSTRACT

The synthesis and characterization of pyridinyl α-diimine Pd(II) complexes having a functionalized hydrocarbon attached to the imino nitrogen was performed. The catalytic activity of these complexes were then evaluated in the polymerization of ethylene and in the Heck coupling reaction of methyl acrylate with iodobenzene.

Unconjugated β-diimine complexes of palladium were also synthesized and their activities towards ethylene polymerization and the Heck coupling of methyl acrylate and iodobenzene also evaluated and compared to that of the α-diimine complexes.

Three of the α-diimine complexes synthesized showed activity towards ethylene polymerization, these being the complexes bearing the allyl, styrene and phenol functionalities. ω-Carboxylato complexes which were also synthesized showed no activity towards ethylene polymerization.

The polymer produced was found to be high density linear polyethylene with an average PDI of 2.54 with M_n values ranging between 3.42 and 6.90 x 10^{-5} and M_w values ranging between 6.05 and 17.6 x 10^{-5}.

The complexes bearing the allyl, styrene and phenol functionalities, as well as the ω-carboxylato complexes active in the Heck coupling reactions of methyl acrylate with iodobenzene.

None of the unconjugated β-diimine complexes prepared showed any activity towards ethylene polymerization even at high Al/Pd ratios. The activity of these complexes towards the Heck arylation reaction was comparable to that of the α-diimine complexes showing similar activities.

ABBREVIATIONS

COD	1,5-Cyclo-octadiene
DAB	Diazabutadiene
DMF	Dimethylformamide
DMSO	Dimethyl sulphoxide
DSC	Differential Scanning Calorimetry
GC-MS	Gas Chromatography-Mass Spectrometry
GPC	Gel Permeation Chromatography
HDPE	High Density Polyethylene
LDPE	Low Density Polyethylene
LLDPE	Linear Low Density Polyethylene
M_n	Number Average Molecular Weight
M_w	Weight Average Molecular Weight
MAO	Methylaluminoxane
MMAO	Modified Methyaluminoxane
NMR	Nuclear Magnetic Resonance
OAc	Acetate
PDI	Polydispersity Index
ppm	Part per million
T_g	Glass Transition Temparture
TGA	Thermal Gravimetric Analysis
THF	Tetrahydrofuran

PUBLICATIONS

CONFERENCE CONTRIBUTIONS:

Oral Presentation : "Synthesis and Applications of Functionalized Pyridinyl Imine Palladium Complexes" , presented at the **Cape Organometallic Symposium, Stellenbosch, South Africa, (2003)**

Poster titled : "The use of Functionalized Diimine Ligands in the Preparation of Palladium Catalyst Precursors for Olefin Polymerization" , presented at the **SACI Inorganic Conference, Pretoria, South Africa, (2003)**

Poster titled : "Catalyst Precursors for Ethylene Polymerization Based On Palladium Complexes Containing Functionalized Diimine Ligands" , presented at the **CATSA Conference, Cape Town, South Africa, (2002)**

TABLE OF CONTENTS

CHAPTER 3 : Catalytic Evaluation of Functionalized Pyridinyl Diimine Complexes of Palladium

Chapter 1

Late Transition Metal Diimine Complexes for Olefin Polymerization

1. Introduction

The revenue generated by the polyolefin industry amounts to multibillions of dollars each year. This translates to a production in excess of 160 billion pounds of which

polyethylene alone contributes approximately 100 billion pounds. Despite this size, the manufacture of polyolefins is a highly technology driven industry.[1] During the past fifty years there have been many rapid advances in the catalysis of olefin polymerization. These include the discovery of heterogeneous Ziegler-Natta catalysts[2], homogeneous early transition metal metallocene catalysts[3], and more recently the development of homogeneous late transition α-diimine ligand systems[4,5].

Three major classes of polyethylene exist (Figure 1.1). High density polyethylene (HDPE) is a linear, semi-crystalline ethylene homopolymer prepared by Ziegler-Natta and chromium catalysts. On the other hand, low density polyethylene (LDPE) is a highly branched ethylene homopolymer prepared in high-temperature and high-pressure free-radical processes. Linear low density polyethylene (LLDPE) is a random co-polymer of ethylene and α-olefins such as 1-butene, 1-hexene or 1-octene and is produced commercially using Ziegler-Natta and metallocene catalysts.

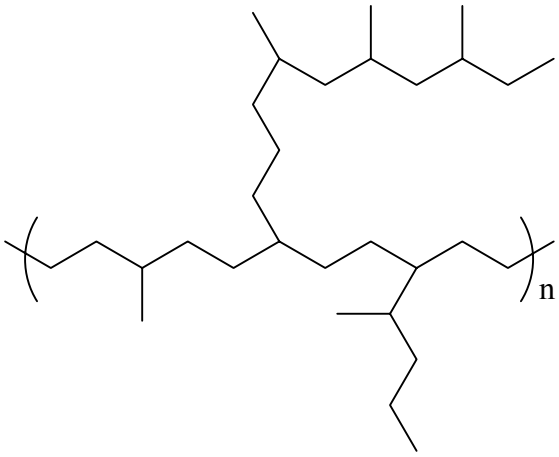

LDPE

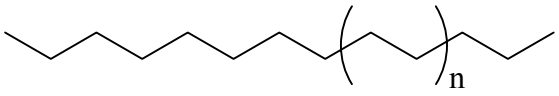

HDPE

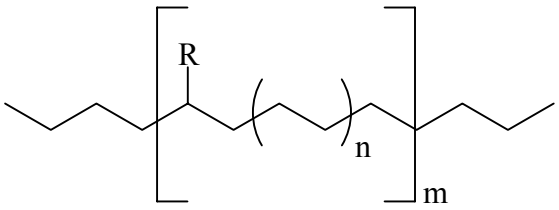

LLDPE

Figure 1.1. The three major classes of polyethylene

Co-polymers of ethylene with functionalized olefins such as methyl (meth)acrylate, (meth)acrylic acid and vinyl acetate are also important commercial polymers.

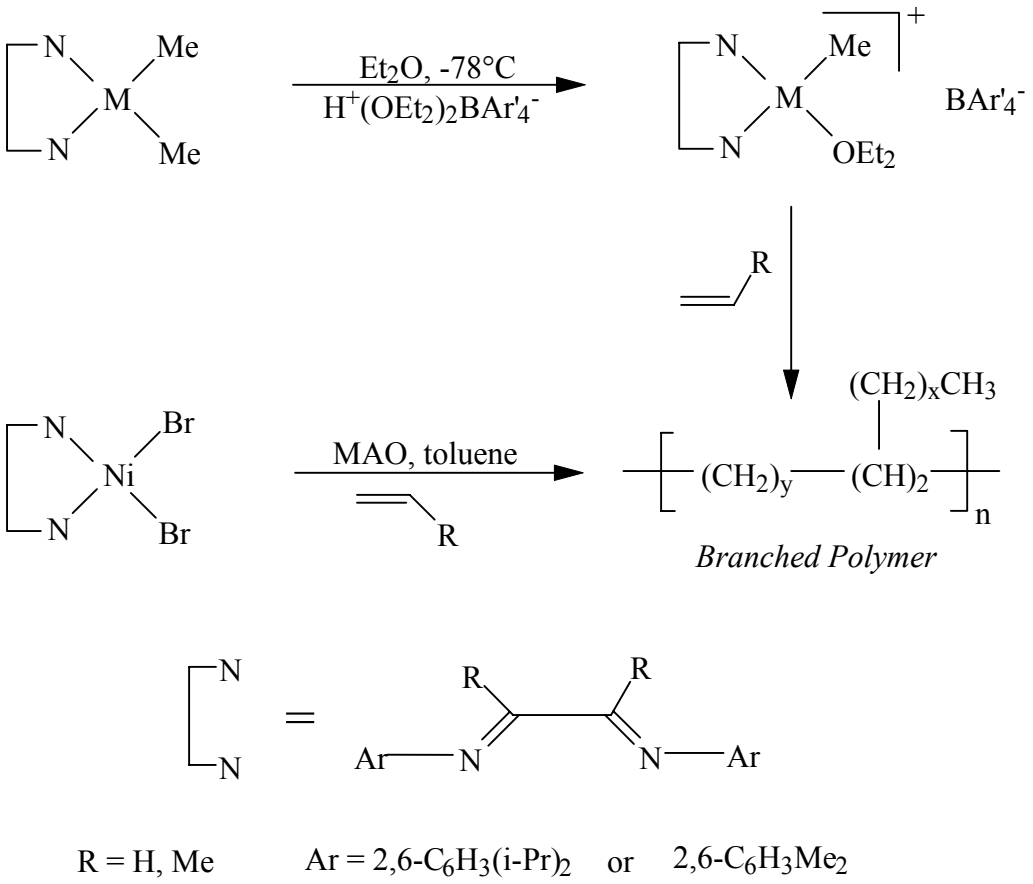

R = H, Me Ar = 2,6-C_6H_3(i-Pr)$_2$ or 2,6-$C_6H_3Me_2$

Scheme 1.3 Protonation of palladium and nickel dimethyl precursors with $H(OEt_2)_2^+BAr'_4^-$

The isolable nickel diethyl ether adducts also catalyzed the polymerization of ethylene and α-olefins and were more conveniently generated *in situ* by methylaluminoxane (MAO) activation of the diimine nickel dibromide complexes in the presence of olefins. The polyethylenes produced by the Ni(II) catalysts ranged from highly linear to moderately branched in which methyl branches predominated. The extent of branching was found to be a function of temperature, ethylene pressure and catalyst structure. Also, these nickel catalysts exhibited extremely high activities which are comparable to those of metallocene catalysts.

1.1 Ziegler-Natta polymerization

Karl Ziegler and co-workers reported in 1955 that solutions of $TiCl_4$ in hydrocarbon solvents in the presence of $Al(C_2H_5)_3$ gave heterogeneous solutions capable of polymerizing ethylene.[2] Many other heterogeneous processes have subsequently been developed for alkene polymerization which utilize aluminum alkyls in combination with transition metal complexes.

A possible mechanism for the Ziegler-Natta process proposed by Cossee[6, 8] and Arlman[7, 8] is given in Scheme 1.1.

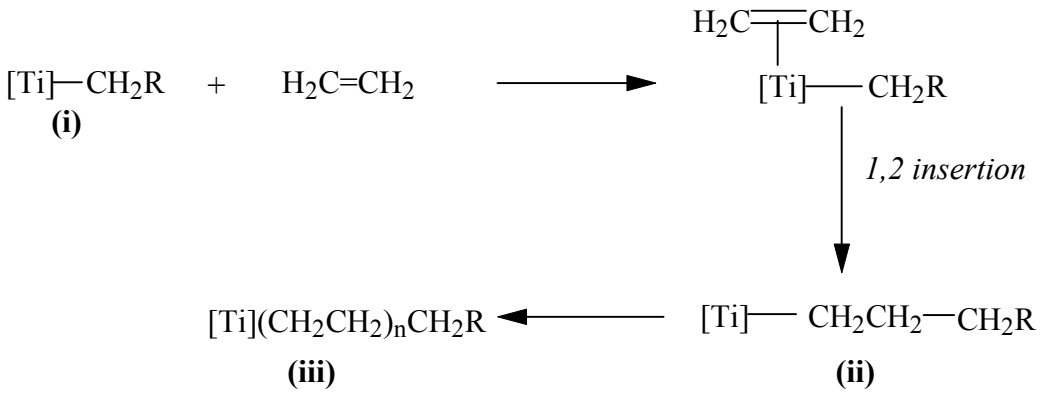

Scheme 1.1 Cossee-Arlman Mechanism [6-8]

Reaction of $TiCl_4$ with an aluminum alkyl gives $TiCl_3$ which on further reaction with the aluminum alkyl gives a titanium alkyl complex **(i)**. Ethylene can then insert into the titanium-carbon bond forming a longer chain alkyl **(ii)**. This alkyl is then further susceptible to insertion of ethylene to lengthen the chain **(iii)**. The Cossee-Arlman

mechanism is supported by studies that demonstrate direct insertions of multiply bonded organic moieties into titanium-carbon bonds[9].

An alternative mechanism involving a metallacyclobutane intermediate has also been proposed and is shown in Scheme 1.2[10].

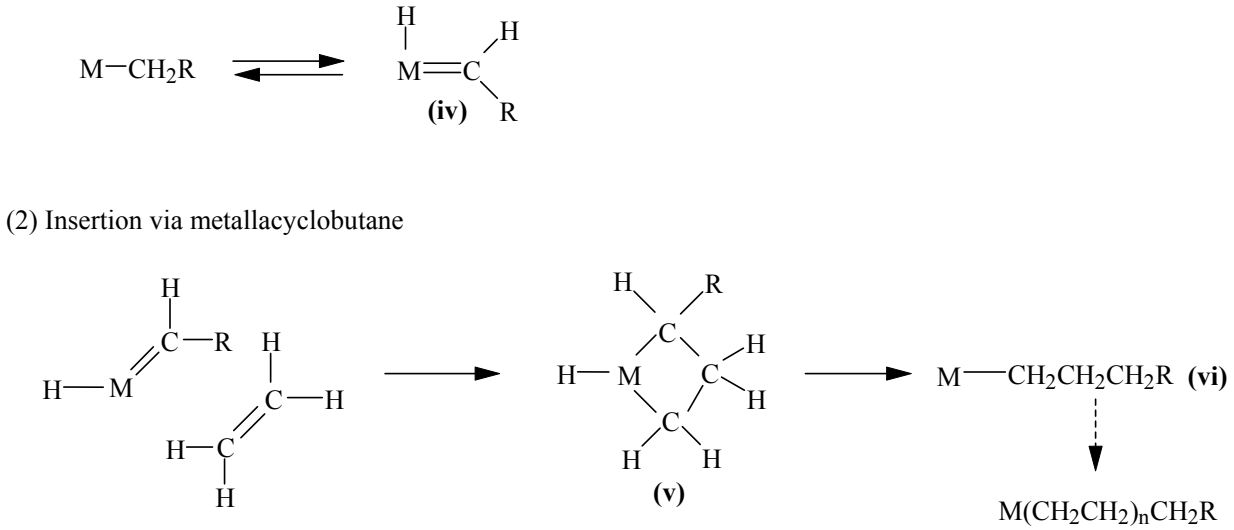

Scheme 1.2 Polymerization via Metallacyclobutane Intermediate

This mechanism involves initial formation of an alkylidiene **(iv)** from a metal alkyl complex. This is followed by addition of ethylene to give the metallacyclobutane **(v)** which then yields the product having ethylene inserted into the original metal carbon bond **(vi).**

Experiments by Grubbs and co-workers have strongly supported the Cossee-Arlman mechanism as the likely pathway for polymerization in most cases[11], but there exists at

least one example that provides evidence that ethylene polymerization occurs via a metallacycle intermediate[12].

Although heterogeneous polymerization catalysts are heavily relied upon in industry, they do have a number of disadvantages. They have for example multiple active sites each having its own rate constants for monomer enchainment, stereoselectivity, co-monomer incorporation and chain transfer[13]. This of course leads to polymers having high polydispersities.

1.2 Homogeneous Early Transition Metal Metallocene Catalysts

In the early eighties, Kaminsky and Sinn found that methylaluminoxane (MAO) resulted in extremely active catalysts when combined with titanium and zirconium metallocenes [14, 15].

Catalysts based on metallocene complexes activated with methylaluminoxane exhibit high activities in olefin polymerization. Also their single site nature makes it possible for the synthesis of polymers having narrow molecular weight distributions and tailored microstructures. This is a significant advantage over Ziegler-Natta catalysts whose structures contain many different active sites. Subsequent advances made in the development of metallocene catalysts have shown that variation of the zirconocene symmetry also strongly influences the resulting polyolefin microstructure[16-19]. Examples of propylene polymerization catalysts to illustrate the relationship between catalyst symmetry and polymer structure are shown in Figure 1.2[20]

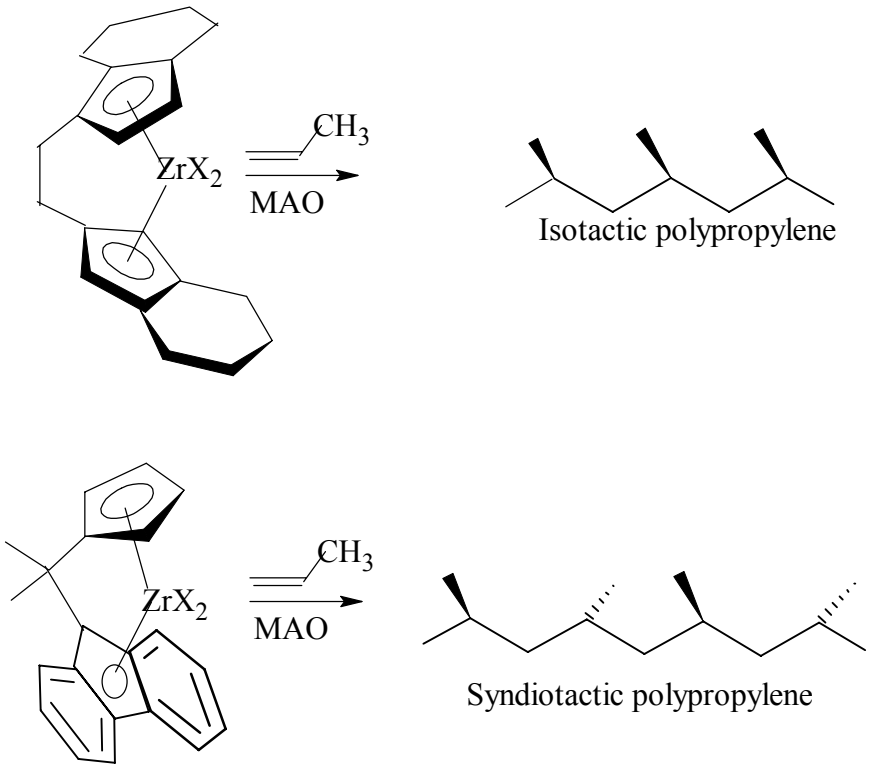

Figure 1.2 Examples of zirconocene catalysts which illustrate the relationship between catalyst symmetry and polymer structure

The disadvantage of these systems however is that the high oxophilicity of early transition metal catalysts causes them to be poisoned by most functionalized olefins. Therefore the lower oxophilicity of and presumed tolerance of late transition metals to functional groups as compared to early transition metals make them likely targets for the development of catalysts for the co-polymerization of ethylene with polar co-monomers under mild conditions.

1.3 Homogeneous Late Transition Metal α-Diimine Catalysts

In 1995 Maurice Brookhart and co-workers reported new Pd(II)- and Ni(II)-based catalysts, which converted both ethylene and α-olefins to high molecular weight polymers with unique microstructures[4]. Until then there had mostly been reports on late transition metal catalysts that dimerize or oligomerize olefins due to β-hydride elimination competing with olefin insertion which occured in these systems. Also, although there were some reports of systems that converted ethylene to high molecular weight polymers, there were no reports on systems that converted α -olefins to polymers with high molar mass.

The Pd(II) and Ni(II) initiators first reported by Brookhart and co-workers were cationic methyl complexes which incorporate bulky diimine ligands[4]. As shown in Scheme 1.3, protonation of the palladium and nickel dimethyl precursors with $H(OEt_2)_2^+ BAr'_4^-$ results in the loss of methane and formation of the diethyl ether adducts. Exposure of the palladium ether adducts to ethylene, propylene or 1-hexene resulted in formation of high molecular weight polymers which were isolated as amorphous materials. These polymers also exhibited extensive branching.

In summary, these Ni and Pd diimine olefin polymerization catalysts developed by Brookhart and co-workers are unique late metal systems capable of converting alpha-olefins to high polymers and were the first systems in which olefin alkyl complexes had been demonstrated to be the catalyst resting states. Also these were the first reported catalyst systems where simple variations in pressure, temperature and ligand substituents allowed access to ethylene homopolymers whose structures varied from highly branched, completely amorphous material to a linear, semicrystalline, high density material.

The three key features of the original α-diimine polymerization catalysts are (1) highly electrophilic, cationic nickel and palladium centres; (2) the use of sterically bulky α-diimine ligands; and (3) the use of noncoordinating counterions or the use of reagents thought to produce noncoordinating counterions. The electrophilicity of the late transition metal centre in these cationic complexes thus results in rapid rates of olefin insertion. The use of bulky ligands therefore favours insertion over chain transfer. Of the three mentioned features, only the use of noncoordinating counterions or of reagents thought to produce noncoordinating counterions seems to be a requirement for late transition metal catalysts. Catalysts having all the mentioned features except steric bulk often tend to be oligomerization catalysts.

Nickel(II) dibromide complexes containing para- and unsubstituted aryl α-diimine ligands in combination with modified methylaluminoxane (MMAO) were also reported by Brookhart *et al* to be highly active and efficient catalysts for the oligomerization of ethylene to linear α-olefins[21]. The oligomers produced were in the C_6-C_{20} range. These

oligomers are feedstocks for the preparation of detergents, plasticizers, fine chemicals, as well as co-monomers for the synthesis of linear low density polyethylene (LLDPE). The easily varied steric and electronic properties of the α-diimine ligands are an important feature of the nickel α-diimine catalyst systems. By eliminating the steric bulk of the ortho-substituents, the rates of associative chain transfer was substantially increased resulting in oligomerization rather than polymerization reactions. The catalyst systems described in Equation 1.1 were examined for ethylene oligomerization. α-Diimine ligands are well known to stabilize organometallic complexes. The synthesis of the ligands involves the condensation of a diketone with two equivalents of an alkyl- or arylamine which were often catalyzed by a Lewis or Bronsted acid. Catalysts **a** and **b** are based on aryl-substituted α-diimines that lack ortho-aryl substituents, and catalyst **c** contains the unsubstituted 2,2'-bipyridine ligand.

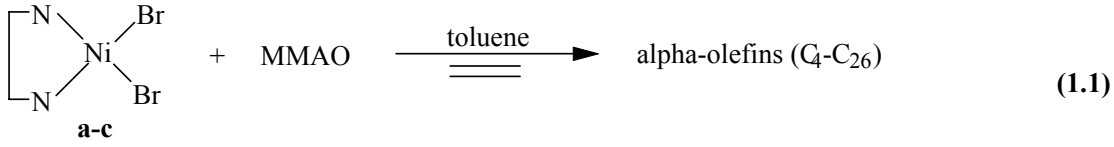

a-c **(1.1)**

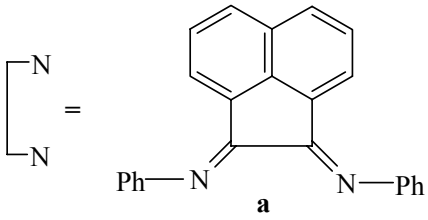

a

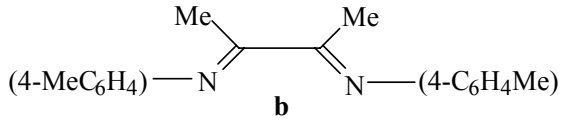

b

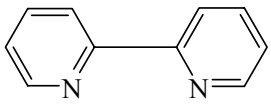

c

1.3.1 Polymerization Mechanism

The polymerization mechanism was investigated by means of NMR studies. This established alkyl olefin complexes as the catalyst resting states. Reaction of the palladium-ether adducts with ethylene at -80°C resulted in the formation of ethylene adducts. A mechanistic rationale for the observations from the NMR studies is presented in Scheme 1.4.

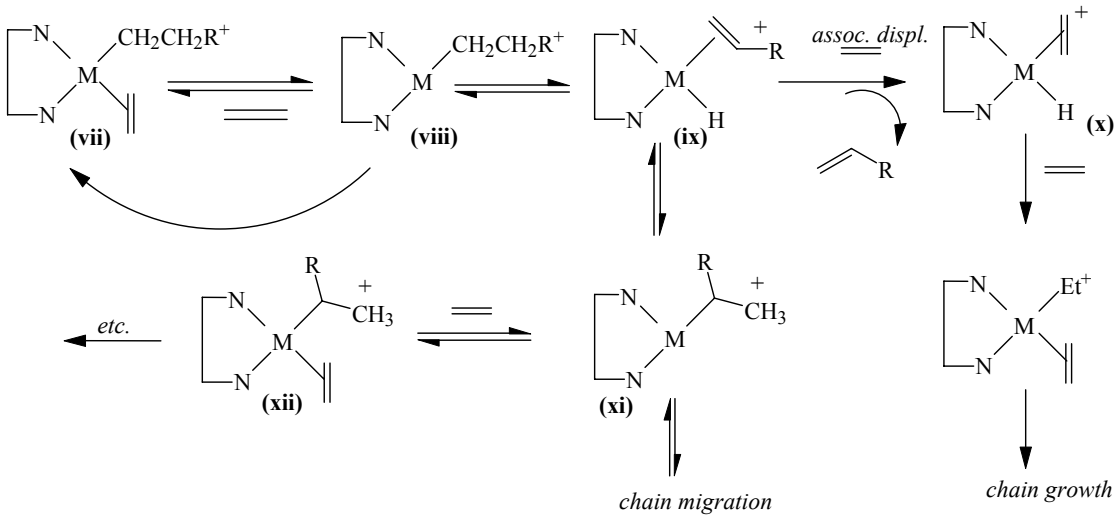

Scheme 1.4 A mechanistic rationale for the observations from NMR studies

The catalyst resting states are alkyl olefin complexes indicated by structure **vii**. Migratory alkene insertion results in **viii**, which can be rapidly trapped by ethylene to reform an alkyl ethylene species. Alternatively, **viii** can also β-hydride eliminate to yield an olefin hydride **ix**. Complex **ix** can undergo reinsertion with opposite regiochemistry, which introduces a branched alkyl group in **xi**. Trapping and insertion of **v** produces a methyl branch, while further chain migration via β-hydride elimination and readdition processes produces longer branches. In a chain transfer process, complex **ix** can release an olefin to

yield **x**, which can initiate a new chain. However, in these M(II) square planar complexes, conversion of **ix** to **xi** must be an associative process, as observed for ethylene exchange in the analogous methyl complexes. The rates of associative displacement and chain transfer (**ix** and **xi**) are greatly retarded by the extreme steric bulk of the diimine ligands. The aryl rings lie roughly perpendicular to the square plane, and the ortho substituents block axial approach of olefins. This feature results in rates of chain propagation which are much greater than chain transfer rates and thus permits formation of high molecular weight polymers.

1.3.2 Co-polymerization with Functionalized Monomers

Brookhart's group also reported on the co-polymerization of ethylene and propylene with functionalized vinyl monomers by palladium(II) catalysts[22]. Until then Ziegler-Natta and related catalysts based on early transition metal d^0 complexes were extensively used for the coordination polymerization of nonpolar olefins such as ethylene and propylene. However, due to their highly oxophilic nature, these catalysts are incompatible with functionalized vinyl monomers. Brookhart and co-workers reported the first examples of metal-catalyzed co-polymerizations of nonpolar olefins (ethylene and propylene) with alkyl acrylates to give high molecular weight polymers using the previously reported late transition metal catalyst systems.

The co-polymerization reactions were initiated by the diethyl ether adducts **f** or the more stable chelate complex **e**, which is easily prepared from **d**, acrylate, and NaBAr'4 (Equation 1.2) and isolated as air and temperature stable solids.

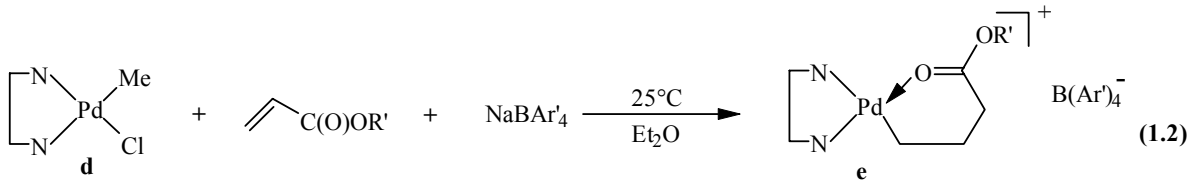

(1.2)

Exposure of **e** or **f** to ethylene or propylene in the presence of alkyl acrylates resulted in the formation of high molecular weight random co-polymers (Equation 1.3).

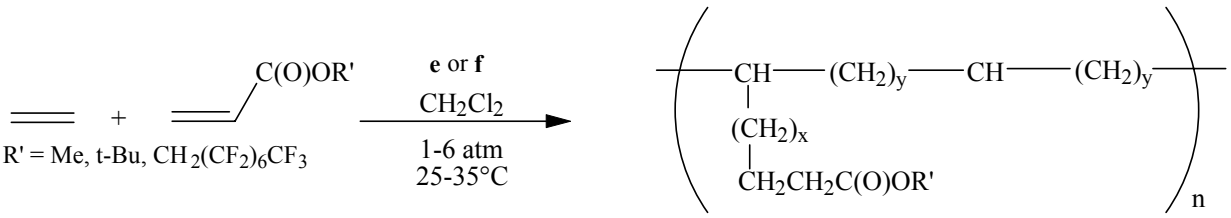

(1.3)

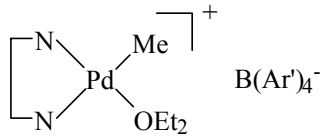

f

Ar' = 3,5-$C_6H_3(CF_3)_2$

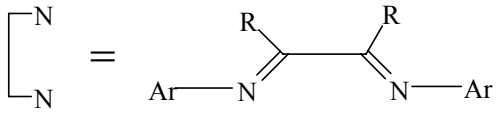

R = H, Me, An Ar = 2,6-C_6H_3(i-Pr)$_2$

(An = CH_2=CH-CN)

It was found using Gel Permeation Chromatography (GPC) that the fraction of acrylate co-monomer was equally distributed over all molecular weights of the monomodal distribution. It was also found that similar to the corresponding ethylene homopolymers, the ethylene co-polymers were amorphous, higly branched materials with approximately

100 branches per 1000 carbon atoms. Typical Tg values fell in the range of -67 to -77°C. The ester groups were also found to be located at the ends of branches in the manner shown in Equation 1.3. Evidence for this was observed from a triplet in the ^{1}H NMR spectrum at 2.2-2.4ppm and a multiplet at 1.6ppm. Similar properties were also observed for an ethylene-methyl vinyl ketone co-polymers and for the amorphous propylene-acrylate co-ploymers.

Productivities of the co-polymerizations were greatly reduced relative to those of the homopolymerizations. Acrylate incorporation was found to be directly proportional to its concentration in the reaction solution and productivity decreased correspondingly.

It was also found that variation of the diimine backbone substituents R did not significantly affect the percentage of acrylate incorporation in the co-ploymer. Productivies were however found to be dependent upon the nature of R (Me > An ≈ H) and followed the same trend as that observed for ethylene homopolymerizations.
These were thus the first transition metal catalysts capable of co-polymerizing ethylene and propylene with polar-functionalized vinyl monomers to high molar mass polymers by a coordination-type polymerization.

1.3.2.1 Mechanism of Co-polymerization with Functionalized Monomers

Low-temperature NMR studies also provided insight into the mechanism of the co-polymerization process (Scheme 1.5).

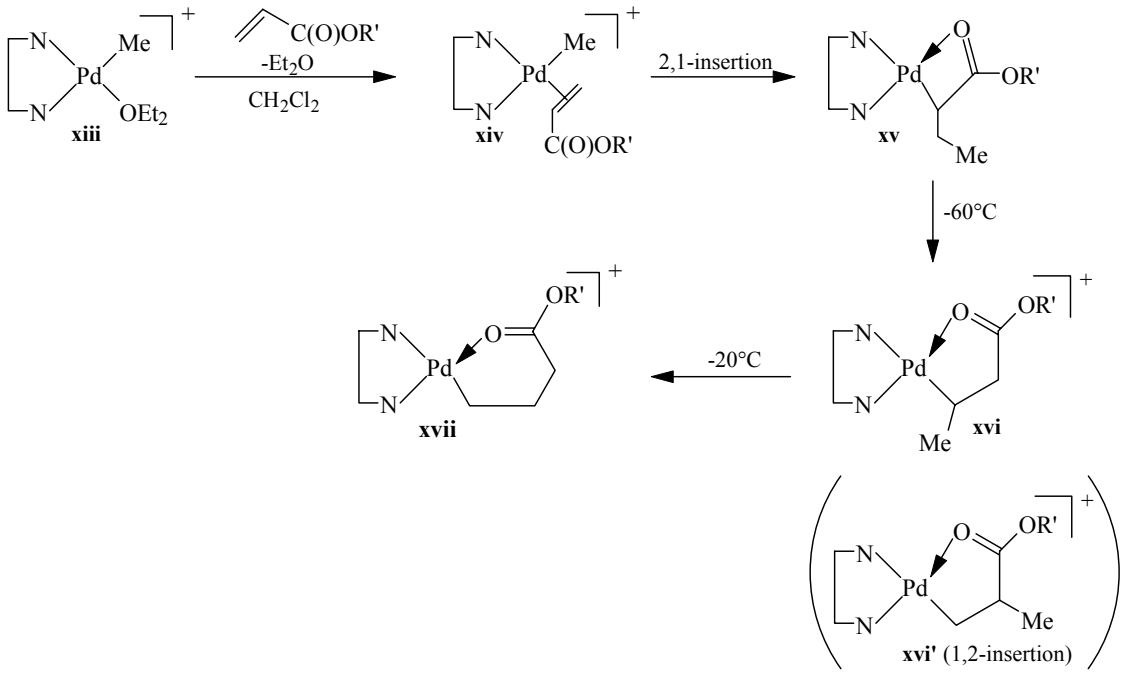

Scheme 1.5 Mechanism of co-polymerization[22]

The reaction of the ether adduct **xiii** with methyl acrylate at -80°C produces the pi-acrylate complex **xiv**, which undergoes 2,1-migratory insertion with ~95% regioselectivity to yield the four-membered chelate **xv**. At -80 to -60°C, complex **xv** isomerizes to the five membered chelate complex **xvi**, which rearranges to the six-membered chelate complex **xvii** at -20°C. Insertion of fluorinated octyl acrylate (FOA) also yields predominantly the six-membered chelate **xvii** as the final product. In contrast, with tert-butyl acrylate, a significant percentage of 1,2-insertion to a give a second five-membered chelate (**xvi'**) also occurs.

Exposure of the ether adduct **xiii** to five equivalents each of ethylene and methyl acrylate at -80°C results in selective formation of the ethylene complex $[(N/\backslash N)PdMe(C_2H_4)]^+$. After complete consumption of ethylene occurs at -30°C, 1 equivalent of methyl acrylate

is incorporated to form a chelate complex analogous to **xvii** by insertion into the Pd-$(CH_2)_{2n}$Me bond. The much more rapid insertion of acrylates into the Pd-R bond (-80°C) than ethylene insertion (-30°C) clearly shows the predominant incorporation of ethylene into the co-polymers is due to the low relative binding constant of methyl acrylate to the electrophilic metal center.

Reversible substitution of the chelating carbonyl group of **e** by ethylene was observed at low temperatures for both the methyl acrylate and FOA chelates (Equation 1.4).

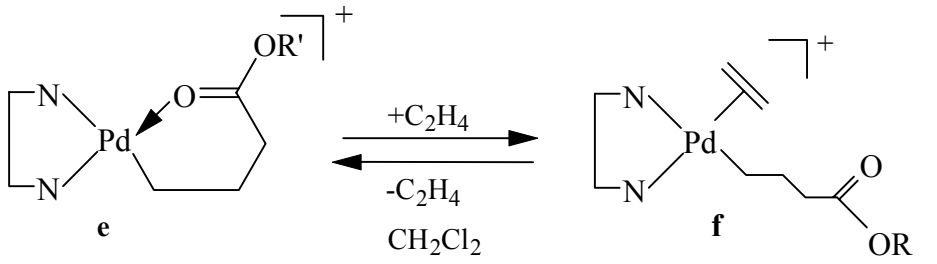

(1.4)

Warming **e** (R' = Me) to temperatures above -30°C results in ethylene polymerization. The only organometallic species observed during this process is **e**, indicating that initiation to form the active species for polymerization is much slower than chain propagation.

The NMR studies and the structure of the co-polymers support the mechanistic pathway depicted in Scheme 1.6.

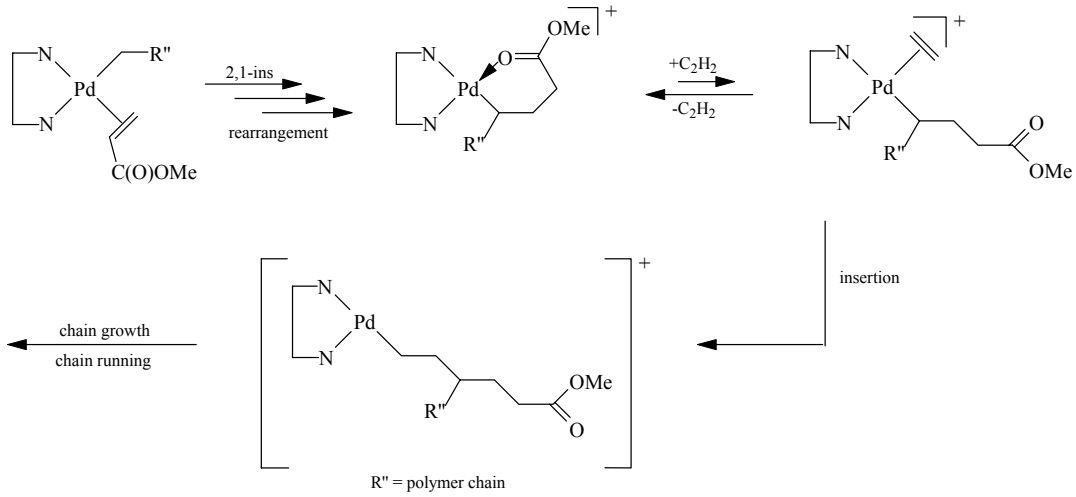

Scheme 1.6 Mechanism of polymerization[22]

During the co-polymerization, a six-membered chelate is formed after insertion of methyl acrylate. Further chain growth requires coordination and insertion of ethylene which is the turnover-limiting step. The chelate complex is thus the catalyst resting state. Therefore, in accordance with the proposed mechanism, raising the ethylene pressure results in an increase in ethylene and methyl acrylate turnovers.

1.3.3 Effect of Ligand Structure on Polymer Properties

As with metallocene catalyst systems, it has been found that ligand structure has an effect on the nature of the resultant polymer. The influence of the ligand structure on the polymerization mechanism is mainly caused by the interaction of subsituents with the axial coordination sites of the metal center. It is especially the steric demands of the substituents which are important. For example, Alt and co-workers reported on the behaviour of α-diimine Ni(II) catalysts that bear halogen substituents at the ligand

framework when used in the polymerization of ethylene[23]. The complexes utilized are summarized in Equation 1.5.

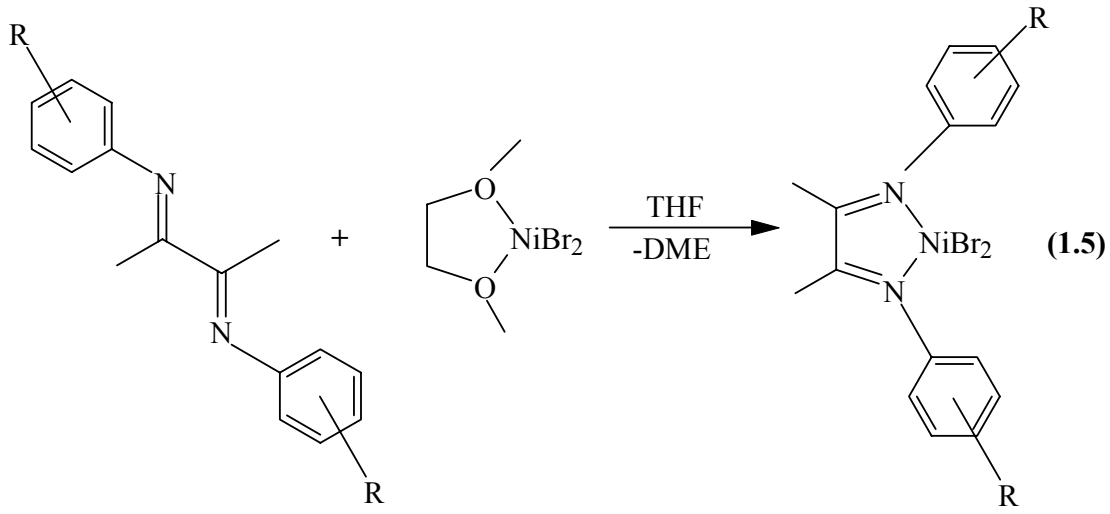

(1.5)

	R
xviiia	**H**
xviiib	**ortho-Me**
xviiic	**para-Me**

	R
xixa	**ortho-F**
xixb	**meta-F**
xixc	**para-F**

	R
xxa	**ortho-Cl**
xxb	**meta-Cl**
xxc	**para-Cl**

	R
xxia	**ortho-Br**
xxib	**para-Br**

	R
xxiia	**ortho-I**
xxiib	**para-I**

The product obtained from the polymerization experiments ranged from low molecular weight oligomers to polymers.

It was also found that in complexes bearing the same substituent, when in the ortho-position the highest activities were observed. The exception were the fluorine containing complexes. In these complexes the one with the para-fluorine substituent exhibited the highest activity. They speculated that an ortho-substituent interacts with the catalytic center via the axial coordination sites of the metal. Therefore, substituents in that position seem to stabilize the active species.

They therefore concluded that the activity of α-diimine Ni(II) catalysts of this type is a correlation between electronic and steric effects caused by the substituents at the aryl moiety of the ligand.

1.3.4 Functionalized α-Diimine Ligand Complexes

To obtain a particular set of polyethylene properties, it is often advantageous to blend two different polymers. This is often achieved through in-reactor blending by combining two nickel or palladium diimine catalysts or by combining a nickel or palladium diimine catalyst with an early transition metal or metallocene catalyst[1]. Functionalised diimine ligand complexes could be used as building blocks to more elaborate systems such as heterobimetallic early/late transition metal complexes. These bimetallic systems could then be used instead of in-reactor blending of catalysts.

Functionalised α-diimine ligands could also be used in the supporting of soluble single-site catalysts on inorganic substrates. This is essential to provide "drop-in" catalysts for

use in existing technologies for slurry or gas-phase polymerization processes. The preparation of supported catalysts through the use of aryl α-diimine Ni(II) complexes substituted with hydroxy or amino functionalities as reactive groups and silica pretreated with trimethylaluminum as activated support material and the use of these supported catalysts for slurry polymerization of ethylene in the presence of various activators has been reported[24]. **Figure 1.3** represents the type of complexes that were supported on the silica.

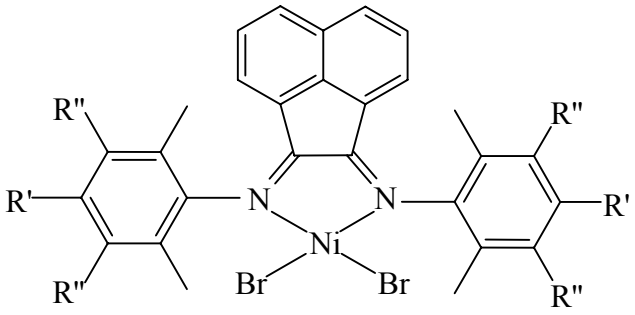

	R'	R"
1	H	H
2	$(CH_2)_3OH$	H
3	CH_2(3,5-Me-Ph)NH_2	H
4	NH_2	Me

Figure 1.3 Types of complexes supported on silica

To support compounds **2**-**4**, methylene chloride solutions of the complexes were combined with the pretreated silica (Scheme 1.9).

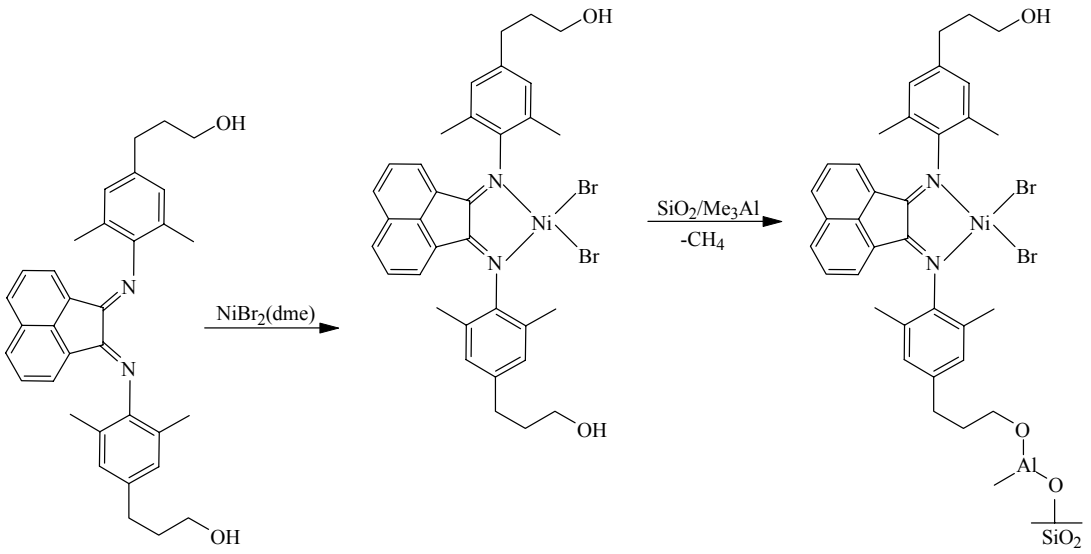

Scheme 1.9 Supporting of compounds **2**-**4** on silica

The supported catalysts were then tested in slurry polymerization runs at 10 atm. ethylene in pentane at temperatures between 30 and 80°C. A polymerization time of 2 hours was chosen to simulate a common residence time in commercial polymerization processes. The Ni(II) diimine complexes covalently attached to silica through hydroxy-functionalized ligands showed very high activities in ethylene polymerization when activated with alkylaluminum halides. With nickel loadings of 0.6wt%, activities up to 750kg of PE/g of Ni were obtained with ethylaluminum sesquichloride (EASC) as co-catalyst.

1.3.5 Other *α*-Diimine Systems

Asymmetrical bidentate aryl substituted pyridylimine-type catalysts have recently been the subject of study by various groups. An example of this is the pyridylimine-type Pd(II)

complexes with a long, straight alkyl group attached to the imino nitrogen reported on by Chen *et al*[25].

Ligands were prepared through the condensation reaction of pyridine-2-carboxaldehyde with the corresponding alkylamines (Equation 1.5).

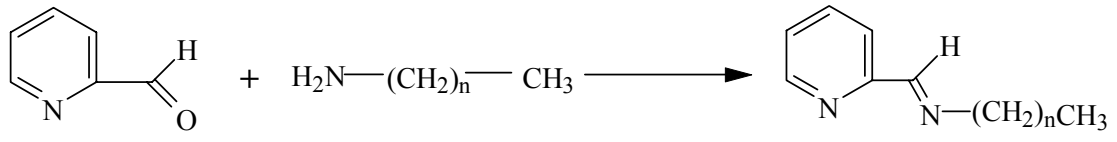

(1.6)

These ligands were then subsequently reacted with (1,5-cyclooctadiene)$PdCl_2$ to afford the desired complexes (Equation 1.6).

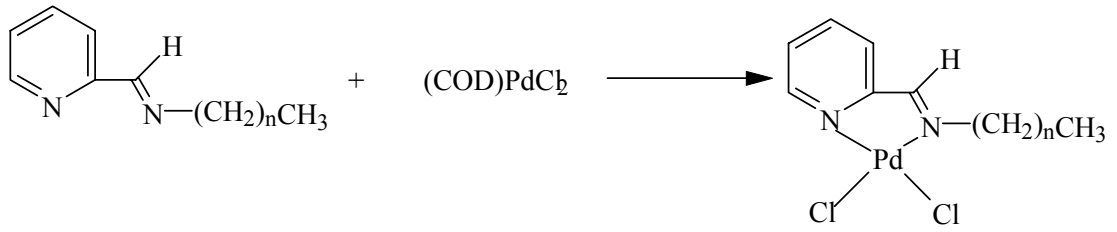

(1.7)

These palladium catalyst precursor systems were shown to produce high molecular weight polyethylene. It was also shown by means of differential scanning calorimetry and ^{1}H and ^{13}C NMR spectroscopy that the polymer produced was high-density linear polyethylene.

They therefore concluded that the co-planar features of the complexes favoured chain propagation and retarded chain transfer and chain running rates. This favours the formation of highly linear polyethylene with high molecular weights. Also the activation reaction of the palladium complexes with methylaluminoxane are affected by the steric features. It also illustrates the effect that the ligand environment has on catalyst activity and polymer microstructure.

1.5 The scope of the thesis

The thesis reports on the synthesis and evaluation of pyridinyl diimine Pd(II) complexes having a functionalized hydrocarbon attached to the imino nitrogen. The purpose of this is to investigate the effect the functionality has on catalyst activity and polymer microstructure. The activities of these functionalized systems are then compared with that of the systems reported on by Chen *et al* which do not contain any functionality[25].

In addition a study of β-diimine complexes of Pd were also carried out and their activities compared to that of the α-diimine systems. Also both types of diimine systems are evaluated for their activity towards Heck coupling reactions.

1.6 References

1. Ittel, S.D, Johnson, L.K., Brookhart, M., *Chem. Rev.*, **2000**, *100*, 1169.
2. Ziegler, K., Holzkamp, H., Martin, H., *Angew. Chem.*, **1955**, *67*, 541.
3. Keim, W., Kowaldt, F.H., Goddard, R., Krüger, C., *Angew. Chem.*, **1978**, *90*, 493.

4. Johnson, L.K., Killian, C.M, Brookhart, M., *J. Am. Chem. Soc.*, **1995**, *117*, 6414.

5. Britovsek, G.J.P., Gibson, V.C., Kimberley, B.S., Maddox, J., McTavish, S.J., Solan, G.A., White, A.P., Williams, D., *Chem. Commun.*, **1998**, 849.

6. Cossee, J., *J. Catal.*, **1964**, *3*, 80.

7. Arlman, E.J., *J. Catal.*, **1964**, *3*, 89.

8. Arlman, E.J., Cossee, J., *J. Catal.*, **1964**, *3*, 99.

9. Eisch, J.J., Piotrowski, A.M., Brownstein, S.K., Gabe, E.J., Lee, F.L., *J. Am. Chem. Soc.*, **1985**, *107*, 7219.

10. Ivin, K.J., Rooney, J.J., Stewart, C.D., Green, M.L.H., *J. Chem. Soc., Chem. Commun.*, **1978**, 604.

11. Clauson, L., Sato, J., Buchwald, S.L., Steigerwald, M.L., Grubbs, R.H., *J. Am. Chem. Soc.*, **1985**, *107*, 3377.

12. Turner, W.H., Schrock, R.R., *J. Am. Chem. Soc.*, **1982**, *104*, 2331.

13. Pino, P., Mülhaupt, R., *Angew. Chem., Int. Ed. Engl.*, **1980**, *19*, 857.

14. Sinn, H., Kaminsky, W., *Adv. Organomet. Chem.*, **1980**, *18*, 99.

15. Kaminsky, W., Miri, M., Sinn, H., Woldt, R., *Makromol. Chem., Rapid Commun.*, **1983**, *4*, 417.

16. Ewan, J.A., *J. Am. Chem. Soc.*, **1984**, *106*, 6355.

17. Kaminsky, W., Külper, K., Brintzinger, H.H., Wild, F.R.W.P., *Angew. Chem., Int. Ed. Engl.*, **1985**, *24*, 507.

18. Ewan, J.A., Elder, M.J., Jones, R.L., Haspeslagh, L., Atwood, J.L., Bott, S.G., Robinson, K., *Makromol. Chem., Macromol. Symp.*, **1991**, *48/49*, 253.

19. Coates, G.W., Waymouth, R.M., *Science*, **1995**, *267*, 217.

20. McKnight, A.L., Waymouth, R.M., *Chem. Rev.*, **1998,** *98*, 2587.

21. Killian, C.M., Johnson, L.K., Brookhart, M., *Organometallics*, **1997**, *16*, 2005.

22. Johnson, L.K., Mecking, S., Brookhart, M., *J. Am. Chem. Soc.*, **1996**, *118*, 267.

23. Helldörfer, M., Milius, W., Alt, H.G., *J. Mol. Cat. A: Chemical*, **2003**, *197*, 1.

24. Preishuber-Pflugl, P., Brookhart, M., *Macromolecules*, **2002**, *35*, 6074.

25. Chen, R., Bacsa, J., Mapolie, S.F., *Polyhedron*, **2003**, *22*, 2855.

Chapter 2

Synthesis and Characterization of Functionalized Pyridinyl Imine Complexes of Palladium

2.1 Introduction

2.1.1 α-Diimine Complexes

The lower oxophilicity and also the presumed greater tolerance of late transition metals to functional groups as compared to early transition metals, have recently made them targets for the development of catalysts for the copolymerization of ethylene with polar comonomers under mild conditions.[1] In 1995, Brookhart and his group reported on new Pd(II) and Ni(II) α-diimine catalysts that were capable of polymerizing ethylene and α-olefins and were also able to polymerize nonpolar olefins with a variety of functionalized olefins.[2, 3] **Figure 2.1** illustrates the types of α-diimine ligands used in the Brookhart catalyst systems.

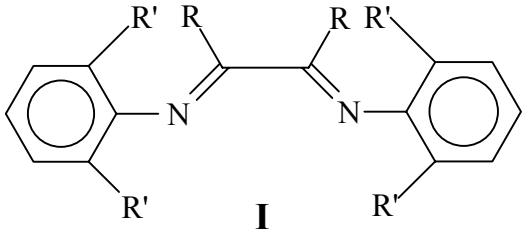

I

I (a) R = H, R' = ^{i}Pr
I (b) R = Me, R' = ^{i}Pr
I (c) R = Me, R' = Me

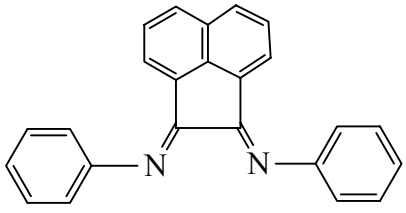

II

Figure 2.1 α-Diimine ligands used in Brookhart catalyst systems

The easily varied steric and electronic properties of the α-diimine ligands are important features of the Ni(II) catalyst systems developed by Brookhart and coworkers. These α-diimine ligands are well known to stabilize organometallic complexes.[4, 5] The synthesis of these ligands involves the condensation of a diketone with two equivalents of an alkyl- or arylamine, often catalyzed by a Lewis or Bronsted acid.

More recently other groups have studied catalyst systems similar to the Brookhart systems but having asymmetrical bidentate arylsubstituted pyridylimine ligands.[6-8] An example of these types of ligands are the pyridinyl-type systems prepared by Chen and coworkers which have long straight alkyl groups attached to the imino nitrogen.[9] These types of ligands are illustrated in **Figure 2.2**.

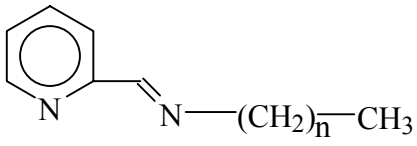

III a: n = 4
III b: n = 7
III c: n = 11

Figure 2.2 Pyridinyl diimine ligands with long straight alkyl groups attached to the imino nitrogen

The synthesis and characterization of ligands and palladium complexes thereof, which are described in this chapter, are similar to those prepared by Chen and coworkers; the main difference being that a functionality is now attached at the end of the alkyl chain.

2.1.2 Unconjugated β-diimine Complexes

The conjugated, monoanionic, β-difunctional ligand shown in **Figure 2.3** is among the most fundamental chelating systems in coordination chemistry.[9] One of its major advantages is its flexibility in synthesis such that a wide variety of terminal substituents R_1 and R_2 and donor atoms or groups X and Y may be incorporated in various combinations.

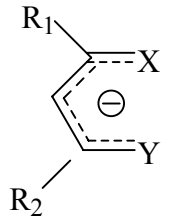

IV

Figure 2.3 General form of conjugated, monoanionic β-difunctional ligand

One such variation of this structure is the β-diiminato ligand shown in **Figure 2.4**.[10] These ligands have been shown to stabilize a wide variety of species with unusual coordination numbers.

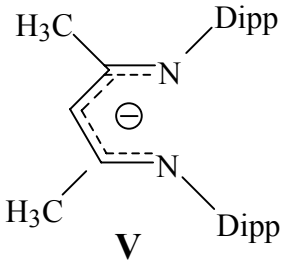

V

Dipp = 2,6- *i* Pr_2-C_6H_3

Figure 2.4 β-diiminato ligand

Coordination of this ligand in its neutral form – β-iminoamine form (**Figure 2.5**) - appears to be rare however.[11] A new class of Ni(II) and Pd(II) catalysts for the polymerization of ethylene and α-olefins using a β-iminoamine ligand **d** was reported by McLain and coworkers though.[12]

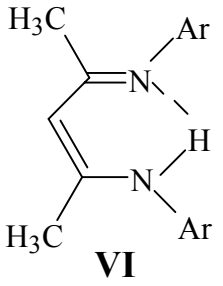

VI

VI a: Ar = C_6H_5
VI b: Ar = Ph-CH_3
VI c: Ar = 2,4,6-$(CH_3)_3$-C_6H_2
VI d: Ar = 2,6-$(iPr)_2$-C_6H_3

Figure 2.5 Neutral β-iminoamine ligand

Recently there has been much interest in α-diimine Ni(II) and Pd(II) alkene polymerization catalyst precursors discovered by Brookhart and coworkers and also in the coordination chemistry of β-iminoamine ligands[13]. This led to a study by Cope-Eatough and coworkers of the synthesis of β-diimine complexes of Pd from β-iminoamines in order to assess the relative activities of α- and β-diimines in the polymerization of alkenes.[14] **Figure 2.6** illustrates the type of complexes synthesized by this group.

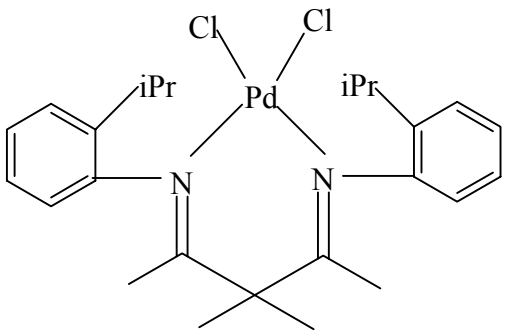

VII

Figure 2.6 β-diimine complex of Pd

It was found however that these β-diimine catalyst precursor systems showed no useful improvement in alkene polymerization as compared to α-diimine complexes of palladium.

In this chapter the synthesis of similar complexes of palladium is described. The difference in this case however is the orientation of the N=C double bond and also the carbon chain length between the two nitrogen atoms. **Figure 2.7** illustrates the type of complexes prepared.

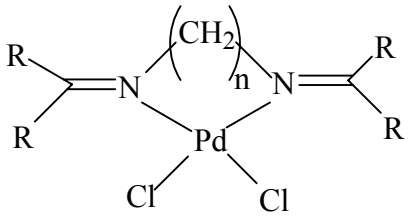

R = aryl or alkyl

n ≥ 1

Figure 2.7 Unconjugated β-diimine ligand complexes of palladium prepared

These complexes were prepared to test their catalytic activity towards ethylene polymerization and compare it to that of conventional β-diimine catalyst precursor systems and also to that of the α-diimine catalyst precursors.

2.2 Synthesis and Characterization of Functionalized Pyridinyl Imine Ligands

2.2.1 Synthesis of Ligands

In general the ligands were synthesized by Schiff base condensation reactions. The synthesis involves the reaction of pyridine-2-carboxaldehyde with the amino derivative of the desired functionalized hydrocarbon using diethyl ether as solvent and anhydrous magnesium sulphate to eliminate the water formed during the reaction. Excess aldehyde was removed by extraction with water. The product was usually isolated as a yellow or orange oil which, if left at room temperature, showed some decomposition over time. The oils were also found to be soluble in most organic solvents such as $CHCl_3$, CH_2Cl_2 and hexane.

The general synthetic route for the ligands is schematically outlined in Equation 2.1.

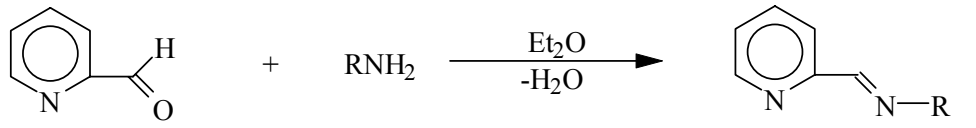

(2.1)

L1; R = $CH_2CH{=}CH_2$
L2; R = $(C_6H_4){=}CH_2$
L3; R = C_3H_7
L4; R = C_5H_{11}

Typically the ligands were obtained in high yields; the lowest yield being approximately sixty percent for the $PhCH{=}CH_2$ ligand. The ligands without any functionality (**L 3** and **L 4**) were prepared to be used in the preparation of complexes that would be evaluated as analogues to the complexes containing a functionality.

In addition to preparing the ligands in Equation 2.1, the synthesis of carboxylic acid functionalized species by reaction of pyridine-2-carboxaldehyde with a C_4 and a C_6 α, ω-amino acid was also attempted. This however did not result in the desired products. It was therefore decided to use the sodium carboxylates of the α, ω–amino acids. The amino acid thus first had to be converted to the corresponding sodium salt, which subsequently was condensed with pyridine-2-carboxaldehyde to give the carboxylate functionalized diimine (**Scheme 2.1**). The condensation reaction to form the ligand was carried out in methanol.

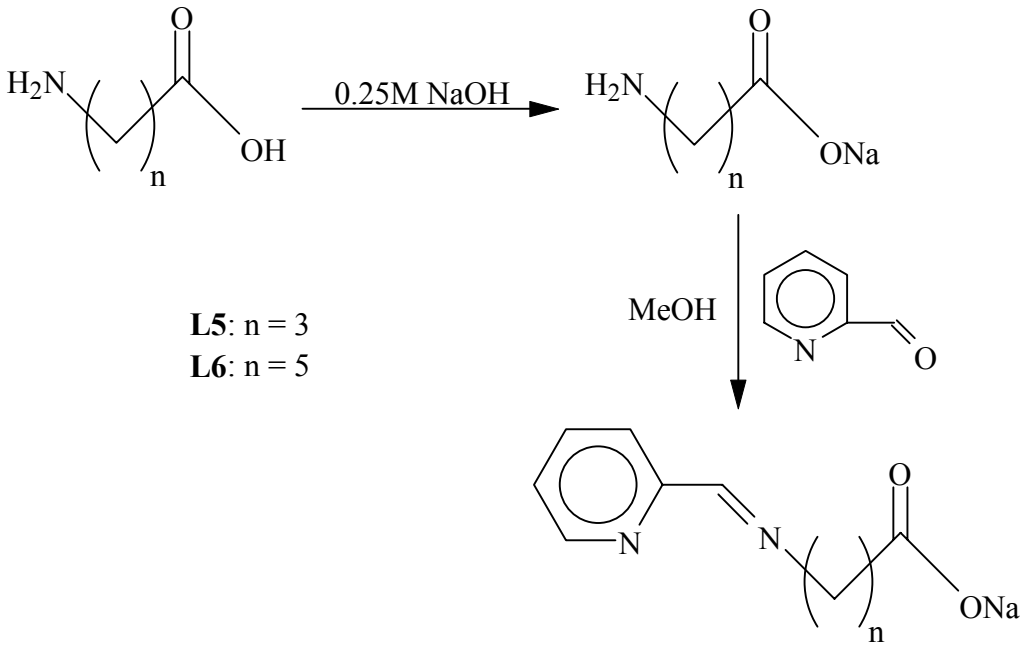

Scheme 2.1 Preparation of sodium carboxylate ligands

After work-up, the products were isolated as pale yellow waxy materials. The work-up involves triturating the initial orange oily residue several times with first acetone and then diethyl ether. This transforms the orange oil into a pale yellow waxy material. The pale yellow waxy material was found to be soluble only in polar solvents such as MeOH, EtOH and H_2O. The product was also found to be hydroscopic on prolonged exposure to air. The ligand was thus stored under vacuum in a Schlenk tube. In both cases yields of about 80% were obtained.

Another modification in the general synthetic route had to be employed for the preparation of the *p*-hydroxyphenyl diimine ligand. The 4-aminophenol starting material was found to be mostly insoluble in organic solvents, being only soluble in H_2O as well as a large excess of tetrahydrofuran (THF). The condensation reaction was thus carried out using THF as solvent. After removal of the solvent under vacuum, the product was isolated as an air stable yellow solid without any further purification. The synthetic route is outlined in Equation 2.2

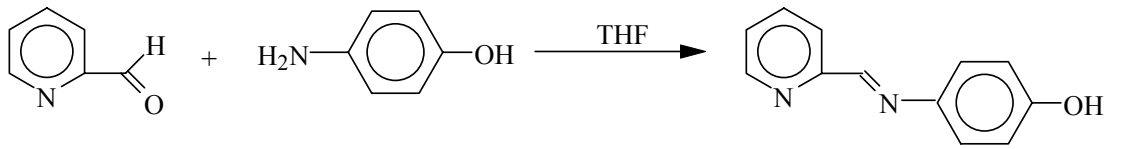

L7 **(2.2)**

2.2.2 Characterization of ligands

The ligands were characterized by ^{1}H and ^{13}C NMR spectroscopy and infrared spectroscopy, as well as elemental analysis.

2.2.2.1 Characterization by means of ^{1}H NMR spectroscopy

The structures of the various ligands as well as their ^{1}H NMR data are shown in **Table 2.1**. The ligands **L3** and **L4** are known compounds prepared by Haddleton and co-workers and their data is included for the sake of comparison[18].

Table 2.1 ^{1}H NMR data of ligands prepared

Ligand	^{1}H NMR Chemical Shift, δ (ppm) (a, b, c)	Assignment
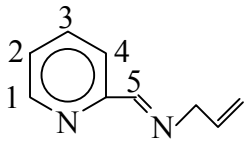 **L1**	δ : 4.16, d δ : 5.04, d δ : 5.90, m δ : 7.18, t δ : 7.56, t δ : 7.87, d δ : 8.25, s δ : 8.51, d	(C**H**$_2$-CH=CH$_2$) (CH=C**H**$_2$) (C**H**=CH$_2$) H-3 H-2 H-4 H-5 H-1
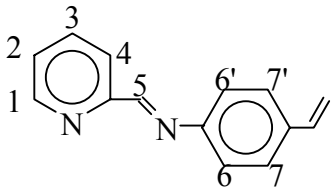 **L2**	δ : 5.20, d δ : 5.71, d δ : 6.70, q δ : 7.27, m δ : 7.42, d δ : 7.71, t δ : 8.14, d δ : 8.58, s δ : 8.65, d	(-CH=C**H**$_2$) (-C**H**=CH$_2$) (-C**H**CH$_2$) H-3 H-7, 7’ H-4 H-2 H-6, 6’ H-5 H-1
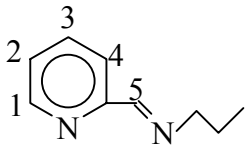 **L3**	δ : 0.88, t δ : 1.67, m δ : 3.56, t δ : 7.22, t δ : 7.65, t δ : 7.91, d δ : 8.30, s δ : 8.56, d	(C**H**$_3$) (CH$_2$C**H**$_2$CH$_3$) (C**H**$_2$CH$_2$CH$_3$) H-3 H-2 H-4 H-5 H-1

a. **L1**-**L4** recorded in $CDCl_3$
b. **L5** recorded in CD_3COCD_3
c. **L6, L7** recorded in D_2O

Table 2.1 continued…

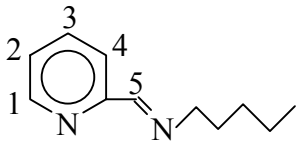 **L4**	δ : 0.86, t	(C**H**$_3$)
	δ : 1.32, m	(C**H**$_2$CH$_3$)
	δ : 1.70, t	(C**H**$_2$CH$_2$CH$_3$)
	δ : 3.63, t	(C**H**$_2$(CH$_2$)$_3$CH$_3$)
	δ : 7.26, t	H-3
	δ : 7.70, t	H-2
	δ : 7.93, d	H-4
	δ : 8.33, s	H-5
	δ : 8.60, d	H-1
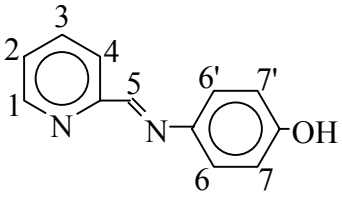 **L5**	δ : 6.61, d	H-7, 7’
	δ : 6.88, d	H-6, 6’
	δ : 7.30, t	H-3
	δ : 7.80, t	H-2
	δ : 8.20, d	H-4
	δ : 8.62, s	H-5
	δ : 8.70, d	H-1
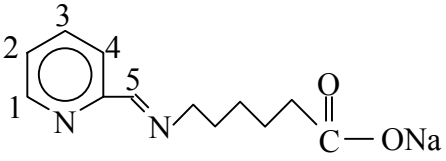 **L6**	δ : 1.34, t	(CH$_2$C**H**$_2$COONa)
	δ : 1.63, m	(CH$_2$(C**H**$_2$)$_2$CH$_2$CO)
	δ : 2.18, t	(NCH$_2$C**H**$_2$)
	δ : 3.66, t	(C**H**$_2$(CH$_2$)$_2$CH$_2$CO)
	δ : 7.50, t	H-3
	δ : 7.86, m	H-2
		H-4
	δ : 8.35, s	H-5
	δ : 8.56, d	H-1
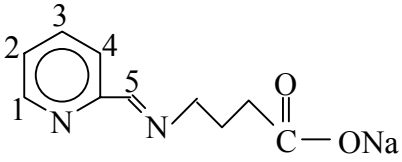 **L7**	δ : 1.99, m	(CH$_2$C**H**$_2$COONa)
	δ : 2.25, t	(NCH$_2$C**H**$_2$)
	δ : 3.70, t	NC**H**$_2$CH$_2$
	δ : 7.50, t	H-3
	δ : 7.93, m	H-2
		H-4
	δ : 8.41, s	H-5
	δ : 8.60, d	H-1

a. **L1-L4** recorded in $CDCl_3$
b. **L5** recorded in CD_3COCD_3
c. **L6, L7** recorded in D_2O

In general, for ligands **L1** to **L4**, the chemical shifts in the aromatic region were found to be similar. **Figure 2.8** illustrates the position of chemical shifts in the aromatic region that are typical of ligands **L1** to **L4**. For each of these ligands there is a doublet at around 8.60 ppm, a singlet at around 8.30 ppm, another doublet at around 7.90 ppm and two triplets; one whose position is between 7.70 and 7.60 ppm and the other whose position is between 7.20 and 7.30 ppm.

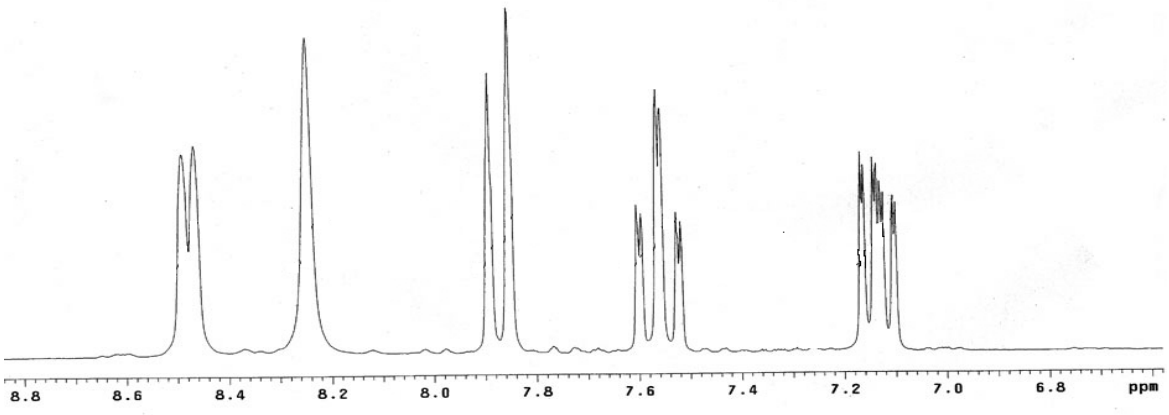

Figure 2.8 Typical chemical shifts in the aromatic region of ligands **L1** to **L4**

Also for **L1** the signals upfield due to the protons of the carbon adjacent to the imino nitrogen give rise to a doublet at 5.04 ppm and the signal due to CH_2 the protons of the vinylic group is a doublet at 4.16 ppm. There is also a multiplet that is due to the CH proton of the vinylic group. These signals are in the expected region for similar vinylic protons.

In the spectrum of ligand **L2** the signals due to the protons of the aromatic ring are found as a quartet at 6.70 ppm. The signal for the CH_2 protons of the vinylic group is a doublet

found at 5.20 ppm and the signal of the single CH vinylic proton is also a doublet found at 5.71 ppm.

In the case of ligand **L3** the signals for the C_3 alkyl chain are found upfield. At 0.88 ppm a triplet due to the CH_3 protons at the end of the chain is observed and at 3.56 ppm another triplet due to the protons on the carbon adjacent to the imino nitrogen is found. There is also a multiplet at 1.67 ppm that is due to the protons on the carbon between the terminal carbon and the one adjacent to the imino nitrogen. These signals are expected to be found in this region, when compared to similar compounds.

With respect to ligand **L4,** signals overlapping at 1.32 ppm and 1.70 ppm are observed. These are due to proton on the central carbons of the C_5 alkyl chain. The signal due to the terminal CH_3 protons is found at 0.86 ppm and the signal due to the proton attached to the carbon adjacent to the imino nitrogen is a triplet found at 3.63 ppm.

For ligand **L5**, the chemical shifts for the aromatic region have the same pattern as for ligands **L1**-**L4**. The signals due to the protons of the aromatic ring are found at 6.61 and 6.88 ppm.

Regarding ligands **L6** and **L7,** it can be seen that the signals of the aromatic protons are in the same region as for ligands **L1** to **L4**, but in the case of the former there is an overlap of the doublet that usually occurs at around 7.90 ppm and the triplet that usually occurs between 7.70 and 7.60 ppm.

The signals due to the protons of the aliphatic carbon chain of ligand **L6** are found upfield. At 1.34 ppm there is a triplet due to the protons of the carbon adjacent to the carboxyl group. The signal due to the protons of the carbon adjacent to the imino nitrogen is also a triplet found at 3.66 ppm. The signal due to the protons of the carbon next to the carbon adjacent to the imino nitrogen is triplet found at 2.18 ppm. A multiplet that is due to the overlapping of the signals due to the protons of the remaining carbons is found at 1.63 ppm.

For ligand **L7** no overlapping of signals occur upfield and there are three distinct signals. At 2.25 ppm there is a triplet due to the protons attached to carbon adjacent to the carboxyl group. The triplet at 3.70 ppm is due to the protons of the carbon adjacent to the imino nitrogen. The signal due to the protons of the central carbon of the alkyl chain is a multiplet found at 1.99 ppm.

2.2.2.2 Characterization by means of ^{13}C {^{1}H} NMR Spectroscopy

Table 2.2 gives the ^{13}C NMR data of ligands **L1**, **L2** and **L5**-**L7**. Signals for all proton decoupled carbons were observed for each ligand synthesized thus giving further evidence that the desired ligands were obtained.

Table 2.2 ^{13}C $\{^{1}H\}$ NMR data of ligands prepared

Ligand	^{13}C NMR Chemical Shift, δ (ppm)	Assignment
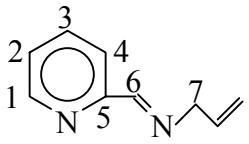 **L1**	δ : 63.15 δ : 116.36 δ : 121.06 δ : 124.59 δ : 135.80 δ : 136.35 δ : 149.27 δ : 154.46 δ : 162.70	C-7 (CH=**C**H_2) C-4 C-2 (**C**H=CH_2) C-3 C-1 C-5 C-6
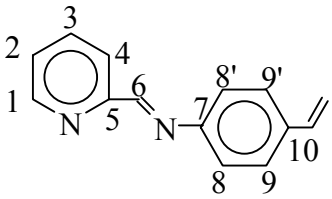 **L2**	δ : 113.03 δ : 120.71 δ : 121.15 δ : 124.34 δ : 126.40 δ : 135.50 δ : 135.59 δ : 135.87 δ : 148.99 δ : 149.65 δ : 153.92 δ : 159.46	(CH=**C**H_2) C-8, 8’ C-4 C-10 C-2 C-9, 9’ (**C**H=CH_2) C-3 C-1 C-7 C-5 C-6
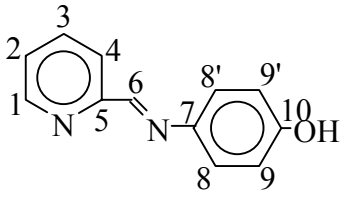 **L5**	δ : 115.77 δ : 120.57 δ : 122.78 δ : 124.85 δ : 136.65 δ : 141.54 δ : 149.39 δ : 154.57 δ : 156.94 δ : 160.11	C-9, 9’ C-4 C-8, 8’ C-2 C-3 C-7 C-1 C-5 C-10 C-6

a. **L1, L2** recorded in $CDCl_3$
b. **L7** recorded in CD_3COCD_3
c. **L5, L6** recorded in D_2O

Table 2.2 continued…

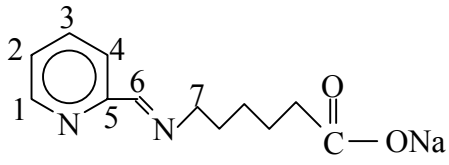 **L6**	δ : 24.65	($NCH_2CH_2\underline{C}H_2$)
	δ : 25.42	($\underline{C}H_2CH_2COONa$)
	δ : 28.49	($NCH_2\underline{C}H_2$)
	δ : 36.60	($\underline{C}H_2COONa$)
	δ : 59.22	C-3
	δ : 120.81	C-4
	δ : 124.90	C-5
	δ : 137.21	C-1
	δ : 147.94	C-2
	δ : 151.44	C-7
	δ : 161.45	C-6
	δ : 182.79	($CH_2\underline{C}OONa$)
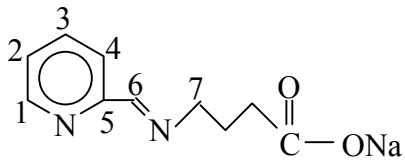 **L7**	δ : 25.73	($NCH_2\underline{C}H_2$)
	δ : 34.16	($\underline{C}H_2COONa$)
	δ : 58.93	C-3
	δ : 121.07	C-4
	δ : 124.94	C-5
	δ : 137.23	C-1
	δ : 147.98	C-2
	δ : 151.36	C-7
	δ : 161.93	C-6
	δ : 181.78	($CH_2\underline{C}OONa$)

a. **L1, L2** recorded in $CDCl_3$
b. **L5** recorded in CD_3COCD_3
c. **L6, L7** recorded in D_2O

The chemical shifts of each signal for the various ligands were found in the expected region after comparison with literature[8].

The chemical shifts of ligands **L6** and **L7** are very similar due to their almost identical structures, **L6** having two extra signals due to the two extra carbons of the alkyl chain as compared to ligand **L7**.

However, when comparing ligands **L2** and **L5** it can be seen that the signals due to C-7, C-8 and C-9 are found at completely different δ(ppm) values despite their near identical structures. This is due to their dissimilar chemical natures imparted to them by their differing functionalities.

2.2.2.3 Characterization by means of Infrared Spectroscopy

For all ligands the infrared spectra each have characteristic bands due to the stretching frequencies of the pyridine ring and C=N bond of the imino group found between 1700 and 1400 cm^{-1} (**Figure 2.9)**. Three bands are observed. An intense band is found at around 1650 cm^{-1} which is due to the C=N bond and two less intense bands at around 1580 and 1450 cm^{-1} due to the pyridine ring.

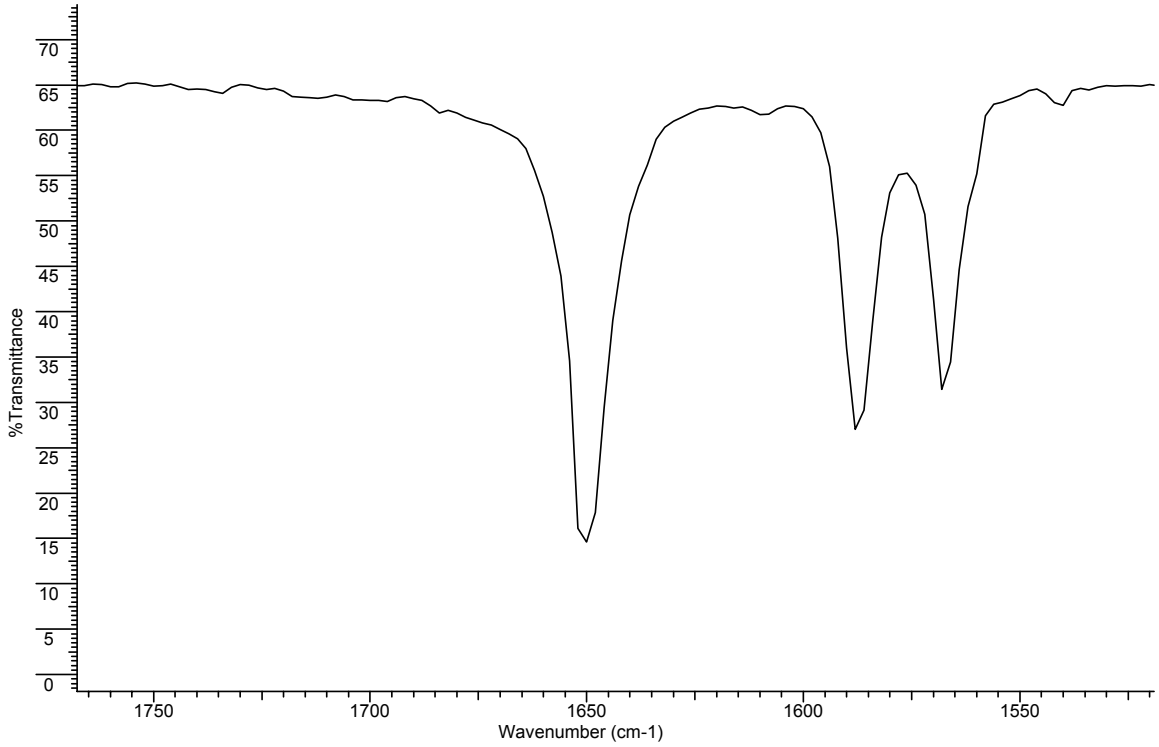

Figure 2.9 IR spectrum showing bands due to the stretching frequencies of the pyridine ring

However, for ligands **L6** and **L7** a broad band in the 1700-1400 cm^{-1} region is observed. This is due to the stretching frequency of the carbonyl group overlapping with the stretching frequencies due to the pyridine ring. **Figure 2.10** illustrates this.

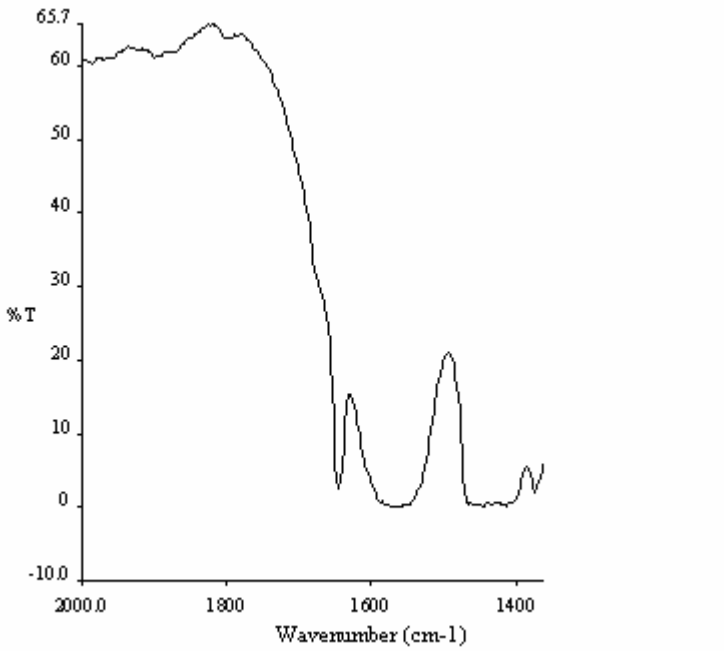

Figure 2.10 IR spectrum of carboxylato ligand showing the overlap of bands

2.3 Synthesis and Characterization of Functionalized Pyridinyl Diimine Complexes of Palladium

2.3.1 Complex Formation

In general the ligands were reacted with either $PdCl_2(COD)$ or $PdCl_2(CH_3CN)_2$ to yield yellow air stable solids. The general synthetic route is outlined in Equation 2.3.

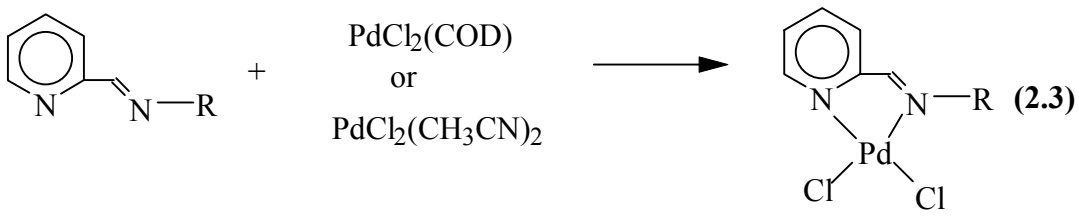

(2.3)

1. R = $CH_2CH{=}CH_2$
2. R = $PhCH{=}CH_2$
3. R = C_3H_7
4. R = C_5H_{11}
5. R = *p*-C_6H_4OH

Complexes **1-4** were found to be insoluble in all solvents other than dimethyl sulphoxide (DMSO). However complex **5** was found to be partially soluble in acetone.

However, when carrying out the complexation of the ω-carboxylato ligands (**L6** and **L7**), different solvents had to be used due to the ligands being soluble only in polar solvents. The complexation was carried out by dissolving the ligand in dry methanol and the $PdCl_2(CH_3CN)_2$ in dry acetone and combining these two solutions. This resulted in the formation of a precipitate that was isolated after removal of the solvents. The resultant pale yellow solids were found to be hydroscopic when exposed to air for long periods of time.

2.3.2 Characterization of Complexes

The complexes were characterized by ^{1}H NMR and ^{13}C NMR spectroscopy, infrared spectroscopy and elemental analysis.

2.3.2.1 Characterization by means of ^{1}H NMR Spectroscopy

The proposed structures of the various complexes as well as their ^{1}H NMR data are shown in **Table 2.3**.

Table 2.3 ^{1}H NMR data of complexes synthesized

Complex	^{1}H NMR Chemical Shift, δ (ppm) (a, b)	Assignment
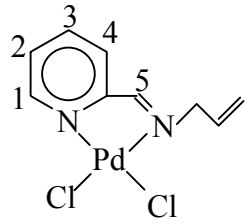 *Complex* **1**	δ : 4.42, d δ : 5.35, t δ : 6.18, m δ : 7.87, t δ : 8.14, d δ : 8.35, t δ : 8.62, s δ : 8.97, d	($CH_2CH=C\underline{\mathbf{H}}_2$) ($C\underline{\mathbf{H}}_2CH=CH_2$) ($NCH_2C\underline{\mathbf{H}}$) H-3 H-4 H-2 H-5 H-1
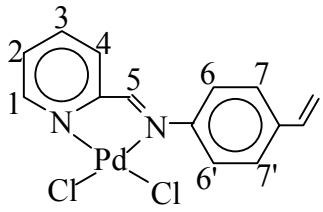 *Complex* **2**	δ : 5.36, d δ : 5.94, d δ : 6.80, q δ : 7.41, d δ 7.57, d δ : 7.94, t δ :8.22, d δ : 8.41, t δ : 8.74, s δ : 9.06, d	($CCH=C\underline{\mathbf{H}}_2$) ($CCH=C\underline{\mathbf{H}}_2$) ($CC\underline{\mathbf{H}}=CH_2$) H-7, 7' H-6, 6' H-3 H-4 H-2 H-5 H-1
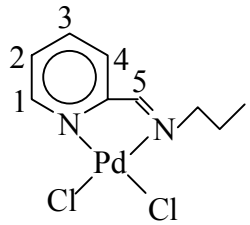 *Complex* **3**	δ : 0.94, t δ : 1.92, m δ : 3.83, t δ : 7.89, t δ : 8.15, d δ : 8.38, t δ : 8.63, s δ : 9.15, d	($CH_2CH_2C\underline{\mathbf{H}}_3$) ($CH_2C\underline{\mathbf{H}}_2CH_3$) ($C\underline{\mathbf{H}}_2CH_2CH_3$) H-3 H-4 H-2 H-5 H-1

a. *Complexes* **1-4** and *Complexes* **6** and **7** recorded in DMSO-d_6
b. *Complex* **5** recorded in CD_3COCD_3

Table 2.3 continued….

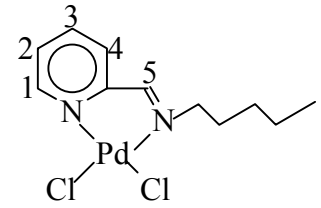 *Complex* **4**	δ : 0.90, t	($C\underline{\mathbf{H}}_3$)
	δ : 1.35, m	($CH_2(C\underline{\mathbf{H}}_2)_3CH_3$)
	δ : 3.86, t	($C\underline{\mathbf{H}}_2(CH_2)_3CH_3$)
	δ : 7.88, t	H-3
	δ : 8.19, d	H-4
	δ : 8.38, t	H-2
	δ : 8.65, s	H-5
	δ : 9.19, d	H-1
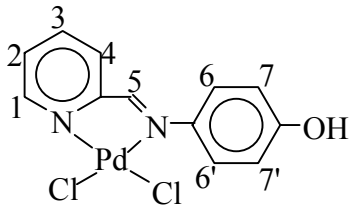 *Complex* **5**	δ : 6.88, d	H-7, 7’
	δ : 7.39, d	H-6, 6’
	δ : 7.89, t	H-3
	δ : 8.23, d	H-4
	δ : 8.40, t	H-2
	δ : 8.64, s	H-5
	δ : 9.23, d	H-1
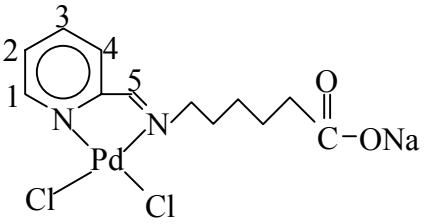 *Complex* **6**	δ : 1.39, t	($CH_2C\underline{\mathbf{H}}_2COONa$)
	δ : 1.67, m	($CH_2(C\underline{\mathbf{H}}_2)_2CH_2COONa$)
	δ : 2.18, m	($NCH_2C\underline{\mathbf{H}}_2$)
	δ : 3.66, t	($C\underline{\mathbf{H}}_2(CH_2)_2CH_2COONa$)
	δ : 6.95, t	H-3
	δ : 7.22, d	H-4
	δ : 7.48, t	H-2
	δ : 7.74, s	H-5
	δ : 8.03, d	H-1
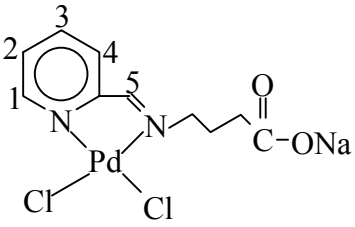 *Complex* **7**	δ : 1.14, t	($CH_2C\underline{\mathbf{H}}_2COONa$)
	δ : 2.14, m	($CH_2C\underline{\mathbf{H}}_2CH_2COONa$)
	δ : 2.82, t	($C\underline{\mathbf{H}}_2CH_2CH_2COONa$)
	δ : 6.99, t	H-3
	δ : 7.23, d	H-4
	δ : 7.50, t	H-2
	δ : 7.80, s	H-5
	δ : 8.02, d	H-1

a. *Complexes* **1-4** and *Complexes* **6** and **7** recorded in DMSO-d_6

b. *Complex* **5** recorded in CD_3COCD_3

A general downfield shift of the aromatic signals was observed upon complexation. A rearrangement of the aromatic signals as compared to the ligand spectra was also observed. For complexes **1-5** a shift of the doublet generally found at around 8.60 ppm assigned to H-1 and the singlet generally found at around 8.30 ppm assigned to H-5 in the ligand spectra is seen in the spectrum of the complex. These two signals move further apart. Also the doublet usually found at around 7.90 ppm assigned to H-4 moves between the two triplets that are usually present in the ligand spectra. **Figure 2.11** illustrates these typical shifting patterns.

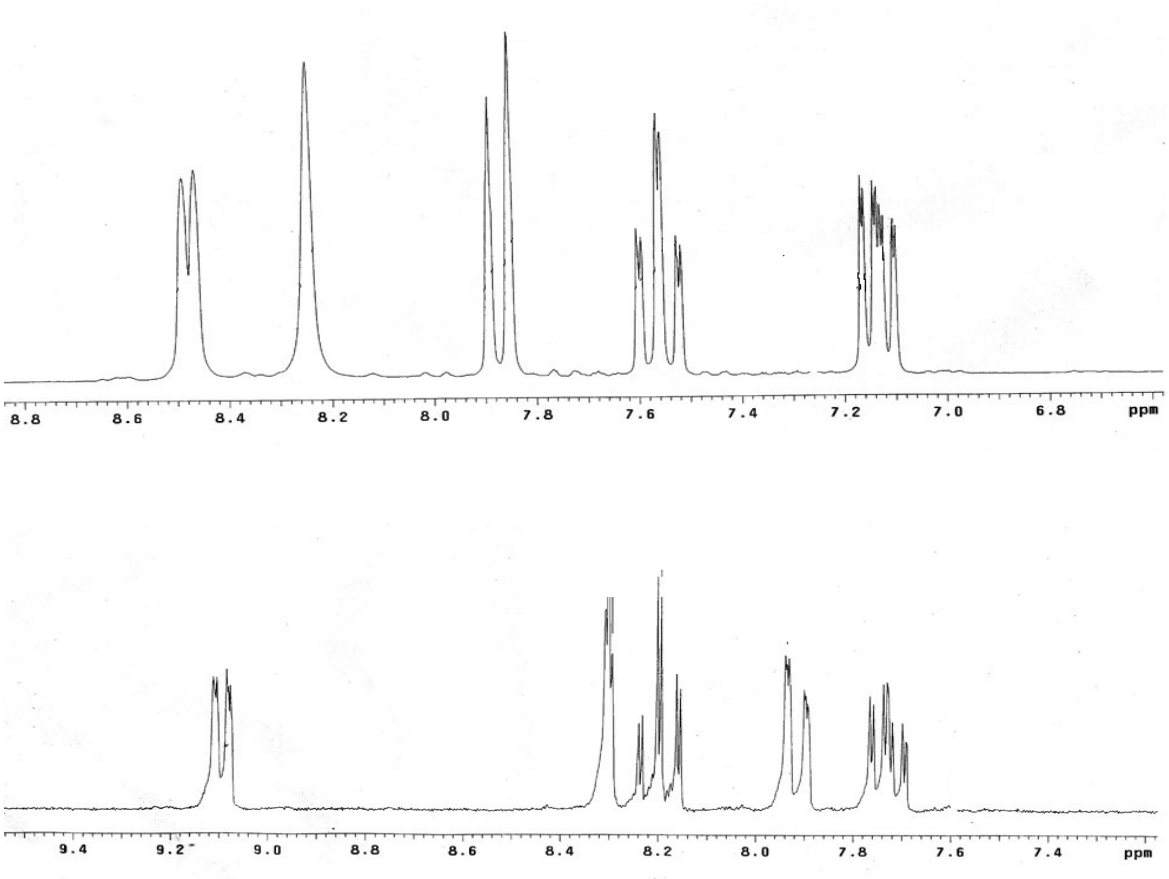

Figure 2.11 Ligand (top) and complex (bottom) ^{1}H NMR spectra showing shifts in signals after complexation

Also, the signals due to proton of the carbon adjacent to the imino nitrogen of all the complexes show an average shift of approximately 1.5 ppm downfield as well. All other signals in the spectra of the complexes are in similar positions as those in the corresponding ligand spectra.

In the case of the carboxylato functionalized ligand complexes (complexes **6** and **7**), the overlapping signals observed in the ligand spectra separate and the signals show the same pattern as observed for complexes **1-5**.

2.3.2.2 Characterization of Complexes by means of ^{13}C {^{1}H} NMR Spectroscopy

The structures of the various complexes as well as their ^{13}C {^{1}H} NMR data are shown in **Table 2.4**. For each complex signals for all proton decoupled carbons are observed. The data thus supports the fact that the expected complexes were obtained.

Table 2.4 ^{13}C $\{^{1}H\}$ NMR data of complexes synthesized

Complex	^{13}C $\{^{1}H\}$ NMR Chemical Shift, δ (ppm) (a, b)	Assignment
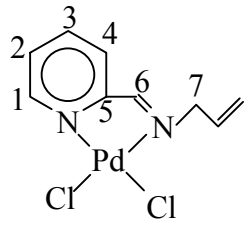 *Complex* **1**	δ : 60.37 δ : 119.83 δ : 128.32 δ : 128.56 δ : 132.96 δ : 141.20 δ : 149.99 δ : 155.73 δ : 171.66	C-7 (CH=**C**H$_2$) C-4 C-2 (**C**H=CH$_2$) C-3 C-1 C-5 C-6
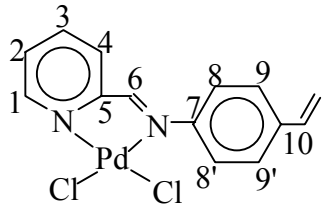 *Complex* **2**	δ : 115.63 δ : 122.82 δ : 123.01 δ : 125.32 δ : 128.23 δ : 136.44 δ : 136.92 δ : 137.20 δ : 151.48 δ : 153.29 δ : 157.33 δ : 163.52	(CH=**C**H$_2$) C-8, 8’ C-4 C-10 C-2 C-9, 9’ (**C**H=CH$_2$) C-3 C-1 C-7 C-5 C-6
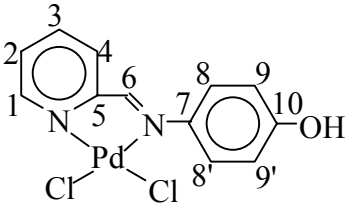 *Complex* **5**	δ : 114.42 δ : 115.78 δ : 122.85 δ : 125.50 δ : 128.46 δ : 136.84 δ : 141.05 δ : 149.84 δ : 157.96 δ : 170.23	C-9 C-9’ C-8, 8’ C-4 C-2 C-3 C-7 C-1 C-5 C-6

a. *Complexes* **1-4** and *Complexes* **6** and **7** recorded in DMSO-d_6

b. *Complex* **5** recorded in CD_3COCD_3

Table 2.4 continued….

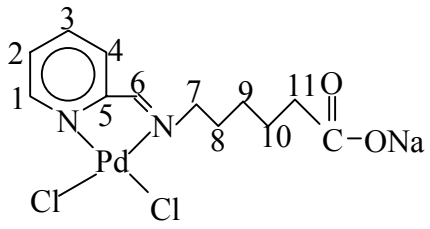

Complex **6**

δ : 21.66	C-9
δ : 23.85	C-8
δ : 25.36	C-10
δ : 34.91	C-11
δ : 55.82	C-7
δ : 127.28	C-4
δ : 128.01	C-2
δ : 141.18	C-3
δ : 149.60	C-1
δ : 154.23	C-5
δ : 170.10	C-6
δ : 182.16	**C**OONa

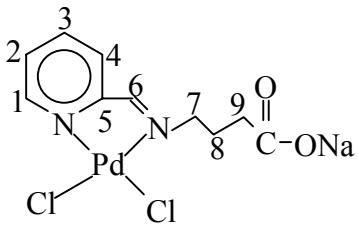

Complex **7**

δ : 25.48	C-8
δ : 30.77	C-9
δ : 58.43	C-7
δ : 128.46	C-4
δ : 128.66	C-2
δ : 141.42	C-3
δ : 150.18	C-1
δ : 156.08	C-5
δ : 171.88	C-6
δ : 173.95	**C**OONa

a. *Complexes* **1-4** and *Complexes* **6** and **7** recorded in DMSO-d_6
b. *Complex* **5** recorded in CD_3COCD_3

2.3.2.3 Characterization by means of Elemental Analysis

Complexes were analyzed for percentage carbon, hydrogen and nitrogen. The results are shown in **Table 2.5**.

Table 2.5 Elemental Analysis results of complexes

Complex	Results	
	Calculated	**Found**
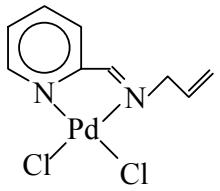 *Complex* **1**	**C:** 33.41% **H:** 3.12% **N:** 8.66%	33.99% 2.99% 8.52%
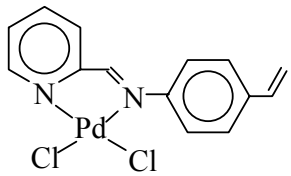 *Complex* **2**	**C:** 43.61% **H:** 3.14% **N:** 7.27%	42.39% 2.89% 6.79%
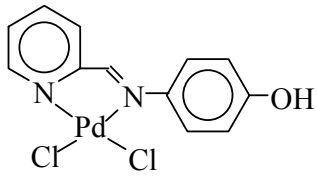 *Complex* **5**	**C:** 38.38% **H:** 2.68% **N:** 7.46%	38.33% 2.25% 6.89%
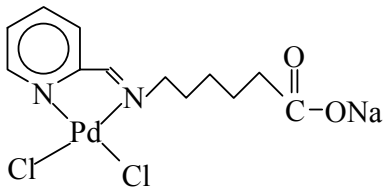 *Complex* **6**	**C:** 34.35% **H:** 3.60% **N:** 6.68%	34.34% 3.32% 6.02%
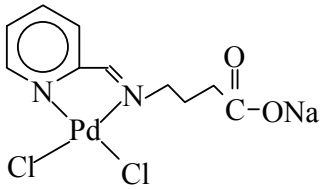 *Complex* **7**	**C:** 30.68% **H:** 2.83% **N:** 7.16%	30.35% 3.08% 6.68%

2.3.2.4 Characterization by means of Infrared Spectroscopy

In the infrared spectra of complexes **1-5** there is a shift of the band at 1650 cm^{-1} to 1600 cm^{-1} as compared to the ligand spectra. This is illustrated by **Figure 2.12**. However the shifting of this band cannot be observed for complexes **6** and **7** since, as in the case of the ligands, there is an overlap of these bands with the band due to the carbonyl stretching frequency which gives rise to a single broad band in this region.

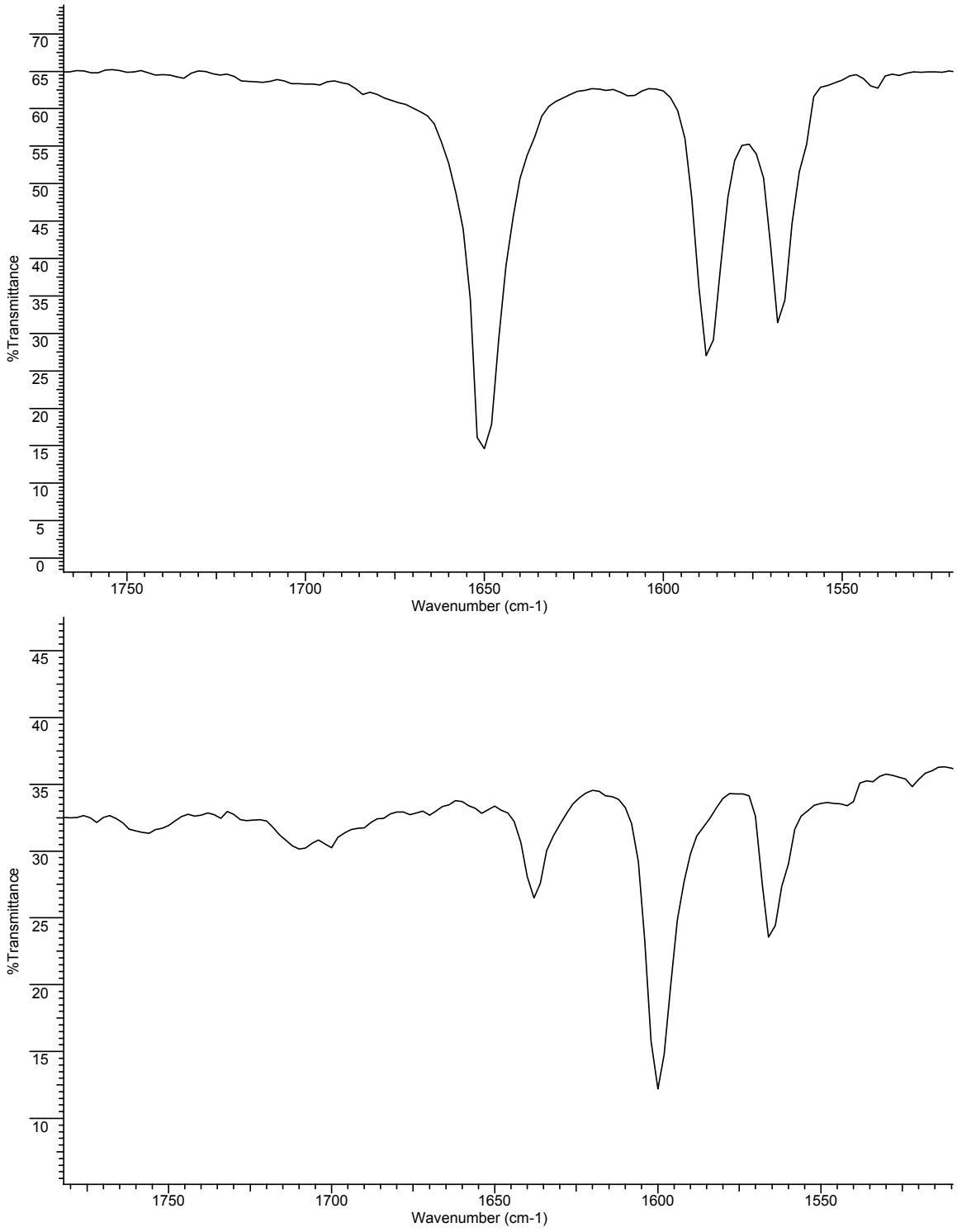

Figure 2.12 Ligand **L1** (top) and Complex **1** (bottom) IR spectra showing change in bands after complexation

2.3.3 Formation of ω-Carboxylato Palladium Complexes using $Pd(OAc)_2$ as Palladium Source

The synthesis of complexes of the ω-carboxylato ligands using $Pd(OAc)_2$ as the palladium source was also attempted. This was done in order to establish whether the solubility of the ω-carboxylato complexes could be improved; the $PdCl_2$ complexes being soluble in only DMSO.

Synthesis was carried out by adding a suspension of the ligand in dry CH_2Cl_2 to the $Pd(OAc)_2$ dissolved in the same solvent. This immediately caused the formation of a pale yellow precipitate. Upon removal of the solvent a hydroscopic yellow solid was obtained. The procedure is schematically outlined in Equation 2.4.

L6 or **L7** suspension in CH_2Cl_2 + $Pd(OAc)_2$ in CH_2Cl_2 ⟶ complex **8** or **9** **(2.4)**

2.3.3.1 Characterization of $Pd(OAc)_2$ Complexes of ω-Carboxylato Ligands

2.3.3.1.1 Characterization by means of ^1H NMR

The ^1H NMR spectra of these complexes are significantly different to the ^1H NMR spectra of complexes **1**-**7**. These differences are most apparent in the chemical shifts observed in the aromatic region in that the same general shift patterns are not observed. For example the separation of the signals due to H-1 and H-5 is not observed. Instead it appears that these two signals swap positions. Also in the case of complexes **6** and **7** there is a separation of the two overlapping signals of the ligand found in the region of 7.8-

8.1ppm upon complexation. However, in the case of the ω-carboxylato ligand complexes, no such separation of signals is observed. The general chemical shift pattern seen for complexes **1** to **5** is thus not observed. **Figure 2.13** illustrates the differences in the ^{1}H NMR spectra of the aromatic region of complexes **8** and **9** as compared to the spectra of complexes **1** to **7**.

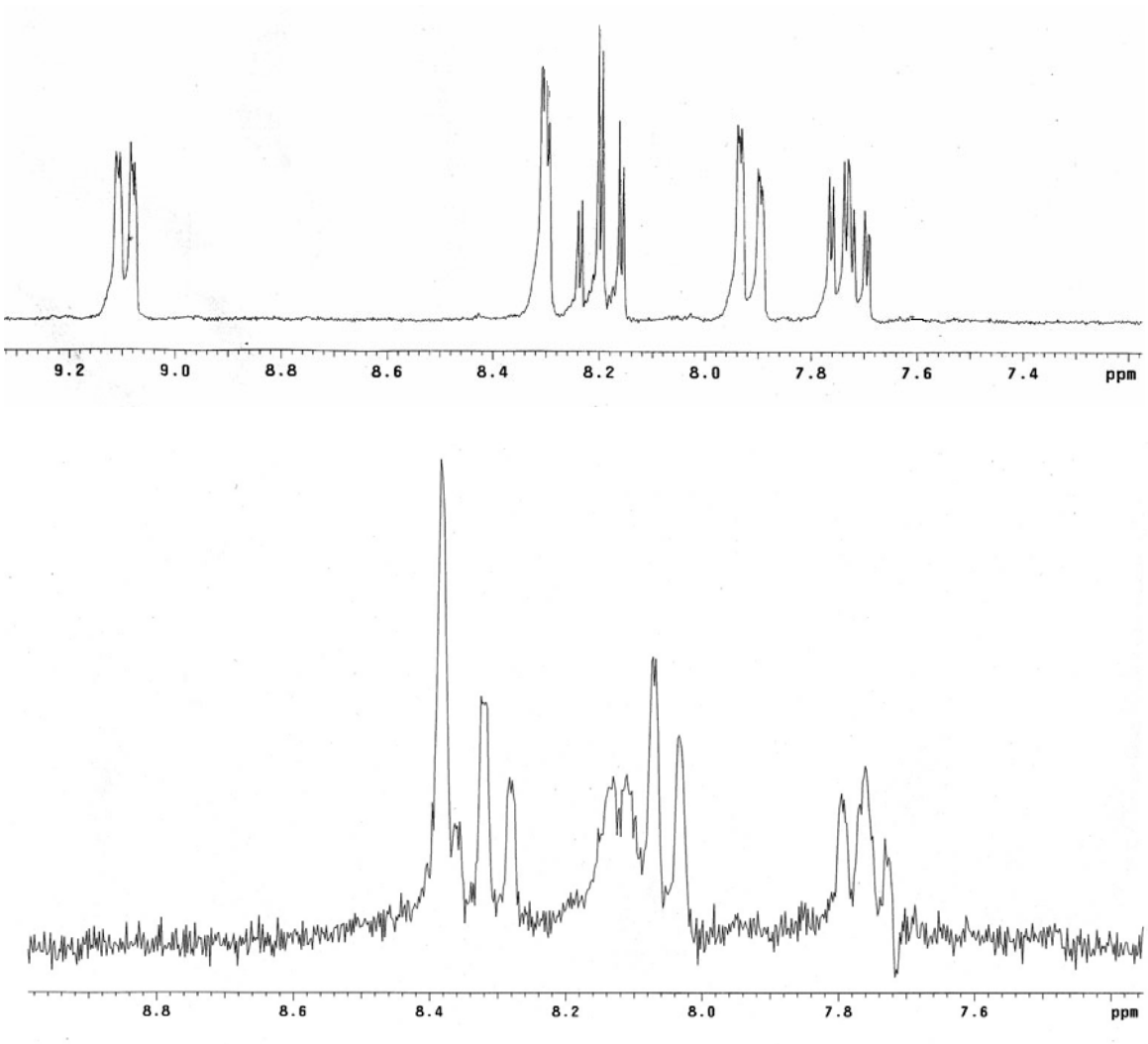

Figure 2.13 ^{1}H NMR spectra of the aromatic region typical of complexes **1** to **7** (top) and of complexes **8** and **9** (bottom) showing differences in shift patterns

Another major difference in the ^{1}H NMR spectra of complexes **8** and **9** is the position of the signal due to the proton attached to the carbon of the alkyl chain adjacent to the imino nitrogen. This signal is found in the same position in the complex spectra as in the corresponding ligand spectra. For complexes **6** to **7** this signal shifts by approximately 1.50 ppm upon complexation of the ligand to the metal. This is not observed in complexes **8** and **9**. What is however observed is that the signal of the protons attached to the carbon adjacent to the carboxyl group show a significant shift (~1.10 ppm) downfield in the complex spectrum as compared to the ligand spectrum. These differences would seem to indicate that the mode of coordination of the ligand to the metal in complexes **8** and **9** is not the same as in complexes **1** to **7**, i.e. the ligand does not coordinate to the metal through the nitrogen of the diimine system.

A possible alternative mode of bonding is shown in **Figure 2.14**. Here the metal is coordinated to the nitrogen of the pyridine ring and the oxygen of the carboxyl group.

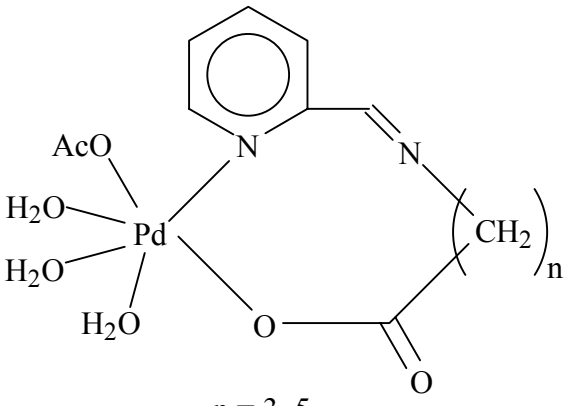

n = 3, 5

VIII

Figure 2.14 Possible mode of bonding in complexes **8** and **9**

This structure could account for the observation of the signal of the proton attached to the carbon of the alkyl chain adjacent to the imino nitrogen not showing a shift downfield as is expected after complexation of the ligand. It could also account for the shift observed for the signal of the proton attached to the carbon adjacent to the carboxyl group after complexation.

Table 2.6 shows the ^{1}H NMR data of complexes **8** and **9**. Data was recorded using D_2O as solvent.

Table 2.6 ^{1}H NMR data of complexes **8** and **9**

Complex	^{1}H NMR Chemical Shift, δ (ppm)	Assignment
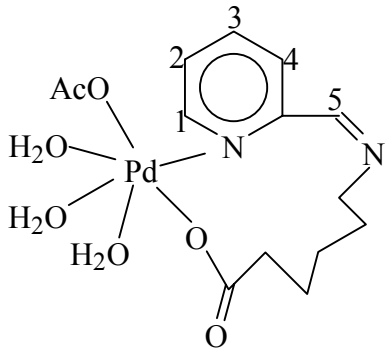 *Complex* **8**	δ : 1.54, m δ : 1.68, m δ : 2.92, t δ : 3.26, t δ : 7.33, t δ : 7.59, m δ : 7.92, m	$((C\underline{\mathbf{H}}_2)_2CH_2COOPd)$ $(NCH_2C\underline{\mathbf{H}}_2)$ $(PdOC\underline{\mathbf{H}}_3)$ $(N(CH_2)_4C\underline{\mathbf{H}}_2COOPd)$ $NC\underline{\mathbf{H}}_2CH_2$ H-2 H-3, H-4 H-1, H-5
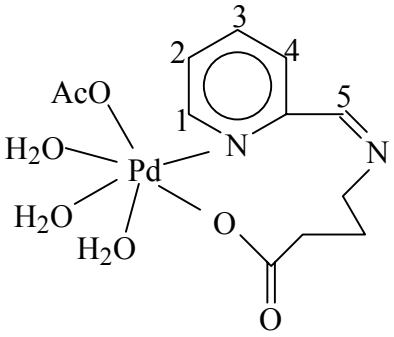 *Complex* **9**	δ : 1.70, m δ : 2.89, t δ : 3.25, t δ : 7.32, t δ : 7.63, m δ : 7.87, m	$(NCH_2C\underline{\mathbf{H}}_2CH_2COOPd)$ $(PdOC\underline{\mathbf{H}}_3)$ $(NCH_2CH_2C\underline{\mathbf{H}}_2COOPd)$ $(NC\underline{\mathbf{H}}_2CH_2CH_2COOPd)$ H-2 H-3, H-4 H-1, H-5

2.3.3.1.2 Characterization by means of Elemental Analysis

From **Table 2.7** it can be seen that the experimental values for the percentage carbon is lower than what was calculated based on the structures shown. This suggests that the structure in which the mode of bonding is the same as for complexes **1** to **7** is incorrect. The elemental analysis results for the complexes which show the alternative mode of bonding are tabulated in **Table 2.8**.

Table 2.7 Elemental Analysis results of complexes **8** and **9** (assuming conventional mode of bonding)

Complex	Results	
	Calculated	**Found**
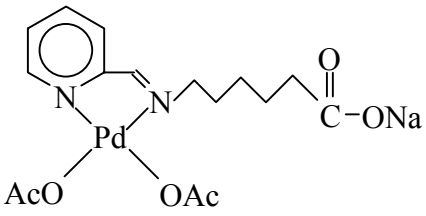	**C:** 43.31%	38.58%
	H: 4.77%	4.85%
	N: 6.31%	5.55%
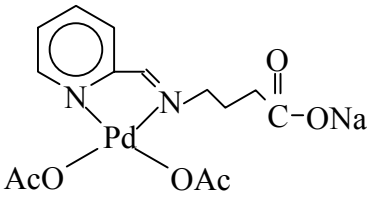	**C:** 40.45%	34.74%
	H: 4.12%	3.98%
	N: 6.74%	5.27%

Table 2.8 Elemental Analysis results for complexes **8** and **9** (alternate mode of bonding)

Complex	Results	
	Calculated	**Found**
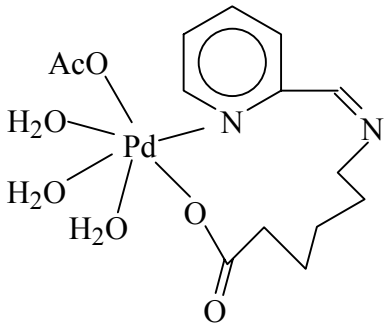 *Complex* **8**	**C:** 38.32% **H:** 5.47% **N:** 6.39%	38.58% 4.85% 5.55%
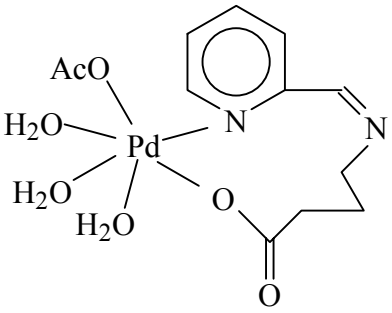 *Complex* **9**	**C:** 35.10% **H:** 4.87% **N:** 6.82%	34.74% 3.98% 5.27%

The experimental elemental analysis results are closer to the calculated results for the alternative mode of bonding (**Figure 2.14**) suggesting these to be the more likely structures of the ω-carboxylato ligand complexes.

2.3.3.1.3 Analysis by means of Thermal Gravimetric Analysis

Complexes **8** and **9** were subjected to Thermal Gravimetric Analysis (TGA) so that the percentage weight lost of the complexes as temperature is increased could be observed. **Figure 2.15** shows the plot of percentage weight versus temperature for complex **8**.

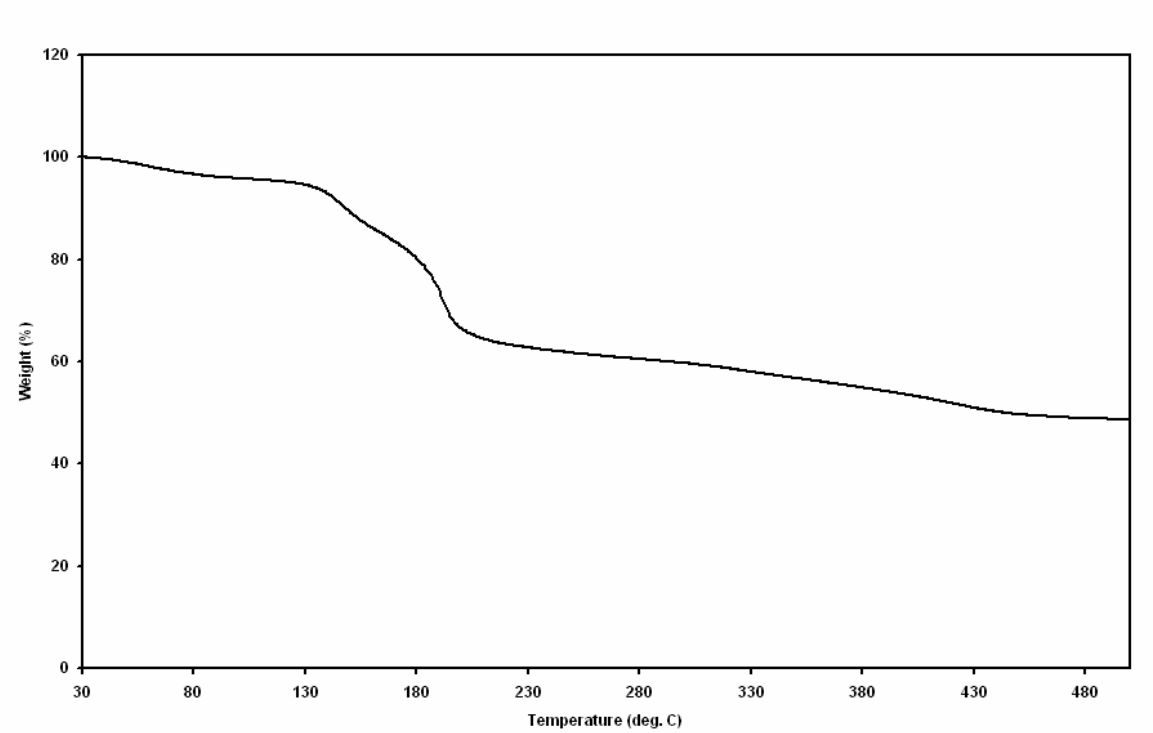

Figure 2.15 Plot of percentage weight versus temperature for complex **8**

A sharp decrease of 24.2% from 30-189°C can be observed for complex **8**. This corresponds to the percentage weight loss (25.8%) of three H_2O molecules and an acetate molecule.

In **Figure 2.16** it can also be seen that there is a sharp decrease of 30% from 30-195°C which corresponds to the percentage weight (27.5%) of three H_2O molecules and the acetate molecule. TGA thus provides further evidence for the structure with water molecules attached to the metal.

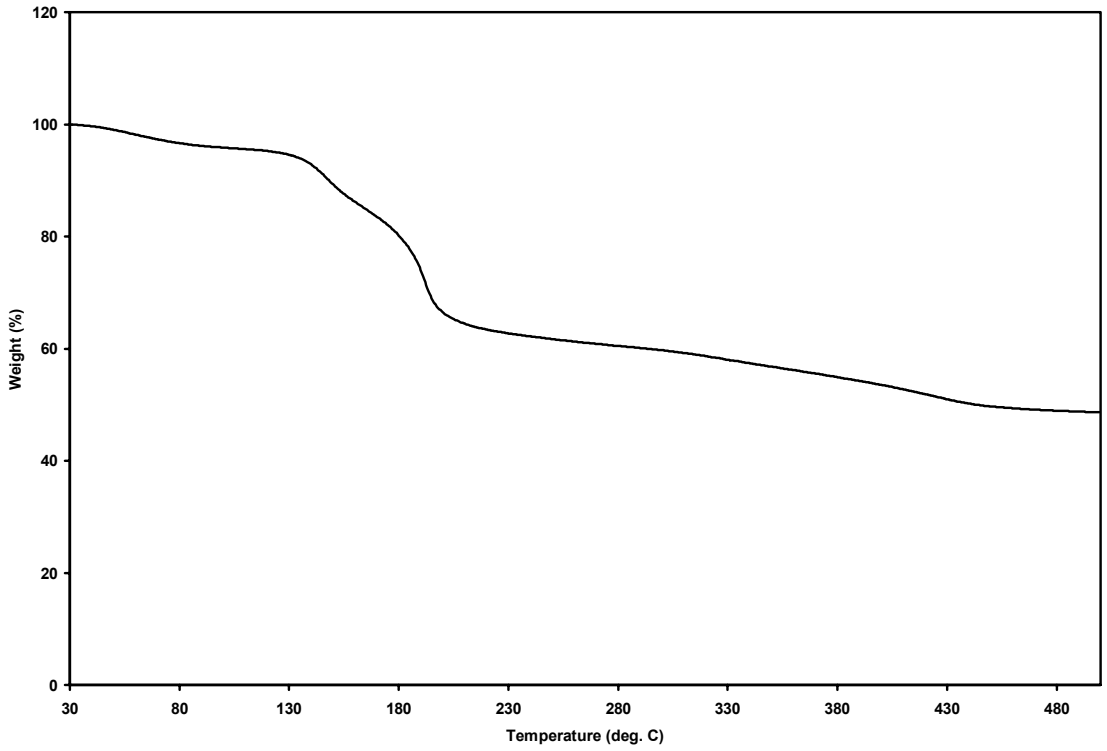

Figure 2.16 Plot of percentage weight versus temperature for complex **9**

2.3.3.1.4 Characterization by means of Infrared Spectroscopy

Further evidence for the suggested alternative mode of coordination of the metal to the ligand can be found by comparing its infrared spectrum with that of a complex exhibiting the normal mode of coordination. In particular one has to compare the regions between 500- and 200 cm^{-1}. Bands in this region would give an indication of whether there are

metal-nitrogen or metal-oxygen stretching frequencies. According to Nakamoto a band due to the Pd-O stretching frequency should be observed at around 420 cm^{-1} [15]. A broad band in this region is indeed observed for complexes **8** and **9** in this region. This broad band is thus due to the Pd-OAc and Pd-OOC stretching frequencies. No such band is observed for other complexes exhibiting the conventional mode of coordination.

2.3.3.1.5 Characterization by means of ^{13}C {^{1}H} NMR Spectroscopy

Table 2.9 gives the ^{13}C {^{1}H} NMR data for complexes **8** and **9**. Signals for all proton decoupled carbons of both complexes are observed. Spectra were recorded using D_2O as solvent.

Table 2.9 ^{13}C {H} NMR data for complexes **8** and **9**

Complex	^{13}C {^{1}H} Chemical Shift, δ (ppm)	Assignment
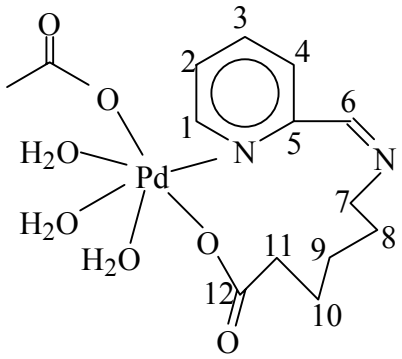 *Complex* **8**	δ : 21.66 δ : 23.85 δ : 24.01 δ : 32.13 δ : 34.91 δ : 55.82 δ : 127.27 δ : 128.01 δ : 141.18 δ : 149.60 δ : 154.23 δ : 170.10 δ : 179.33 δ : 182.16	C-8 C-9 C-10 C-11 ($C\underline{\mathbf{H}}_3COO$) C-7 C-4 C-2 C-3 C-1 C-5 C-6 C-12 $CH_3(\underline{\mathbf{C}}OOPd)$
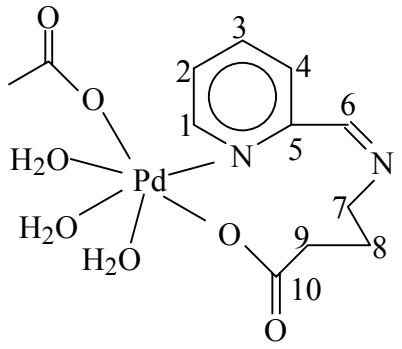 *Complex* **9**	δ : 21.58 δ : 23.85 δ : 34.90 δ : 55.83 δ : 127.26 δ : 127.98 δ : 141.17 δ : 149.60 δ : 154.24 δ : 170.10 δ : 179.02 δ : 182.18	C-8 C-9 ($C\underline{\mathbf{H}}_3COO$) C-7 C-4 C-2 C-3 C-1 C-5 C-6 C-10 $CH_3(\underline{\mathbf{C}}OOPd)$

2.4 Synthesis and Characterization of Unconjugated β-Diimine Complexes of Palladium

2.4.1 Ligand Synthesis

The general synthesis involves reacting two mole equivalents of benzophenone with one molar equivalent of the appropriate diamine with the desired carbon chain length[16]. Equation 2.5 outlines the general synthetic procedure.

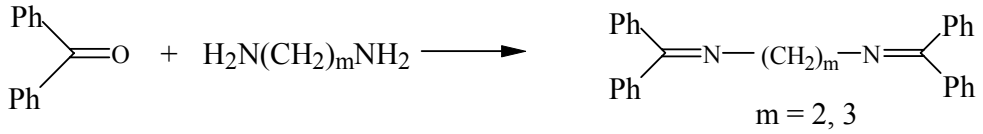

(2.5)

L9, m = 2
L10, m = 3

Products were isolated as air stable white crystals after recrystallization from heptane.

2.4.1.1 Characterization of Ligands by means of ^{1}H NMR

Table 2.10 gives the ^{1}H NMR data of the synthesized ligands. The spectra were recorded using $CDCl_3$ as solvent.

Table 2.10 ^{1}H NMR data of unconjugated β-diimine ligands synthesized

Ligand	^{1}H NMR Chemical Shifts, δ (ppm)	Assignment
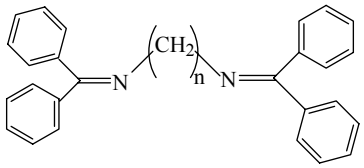 n = 2 **L8**	δ : 3.76, s δ : 7.42, m	(N(C**H**$_2$)$_2$N) (C$_6$**H**$_5$)
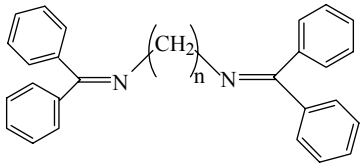 n = 3 **L9**	δ : 2.23, t δ : 3.61, t δ : 7.52, m	(NCH$_2$C**H**$_2$CH$_2$N) (NC**H**$_2$CH$_2$C**H**$_2$N) (C$_6$**H**$_5$)

For ligand **L8** two signals are observed; a multiplet in the aromatic region and a singlet for the four equivalent protons attached to the carbons adjacent to the imino nitrogen. For ligand **L9** three signals are observed; a multiplet for the protons of the phenyl, a triplet for the four equivalent protons of the carbons attached to the carbons adjacent to the imino nitrogens and a triplet for the protons attached to the central carbon of the alkyl chain.

2.4.2 Synthesis and Characterization of Unconjugated β-Diimine Complexes of Palladium

Complexes **10** and **11** were formed by reacting ligands **L8** and **L9** with $PdCl_2(CH_3CN)_2$ under an atmosphere of purified nitrogen using dry acetone as solvent. Products were isolated as yellow solids after washing with acetone. Equation 2.6 schematically outlines the procedure. The products were found to be sparingly soluble in both $CHCl_3$ and CH_2Cl_2. Complex **11** was also found to be soluble in DMSO whereas complex **10** was not.

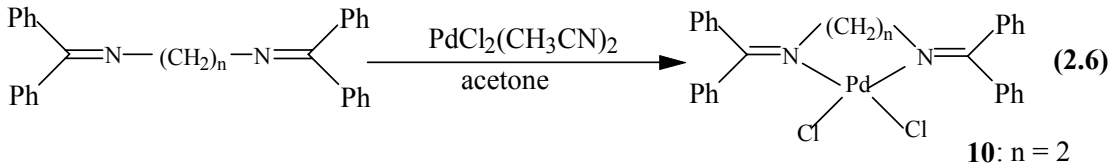

(2.6)

10: n = 2
11: n = 3

2.4.2.1 Characterization of Complexes

Complexes were characterized by ^{1}H NMR spectroscopy, infrared spectroscopy and elemental analysis.

2.4.2.1.1 Characterization by means of ^{1}H NMR Spectroscopy

Table 2.11 gives the ^{1}H NMR data of complexes **10** and **11**. The ^{1}H NMR spectrum of complex **10** was recorded in $CDCl_3$ and that of complex **11** in DMSO.

Table 2.11 ^{1}H NMR data of complexes **11** and **12**

Complex	^{1}H NMR Chemical Shifts, δ (ppm)	Assignment
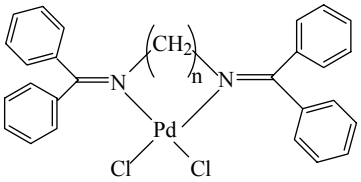 n = 2	δ : 4.15, s δ : 7.53, m	(N(C**H**$_2$)$_2$N) (C$_6$**H**$_5$)
Complex **10**		
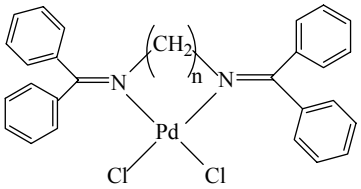 n = 3	δ : 2.51, t δ : 3.88, t δ : 7.65, m	(NCH$_2$C**H**$_2$CH$_2$N) (NC**H**$_2$CH$_2$C**H**$_2$N) (C$_6$**H**$_5$)
Complex **11**		

The ^{1}H NMR spectra of complexes **10** and **11** are similar to that of the free ligands, the only difference being the expected shift downfield of the signals due to the protons attached to the carbons of the alkyl chain.

2.4.2.1.2 Characterization by means of Infrared Spectroscopy

Figure 2.16 shows the comparative spectra of ligand **L8** and complex **10.** For complex **10** there is a shift of the band at 1050 cm^{-1} in the ligand spectrum to 1000 cm^{-1} in the complex spectrum. This is similar to what happens when comparing the infrared spectra of the α-diimine ligands with their corresponding complex infrared spectra.

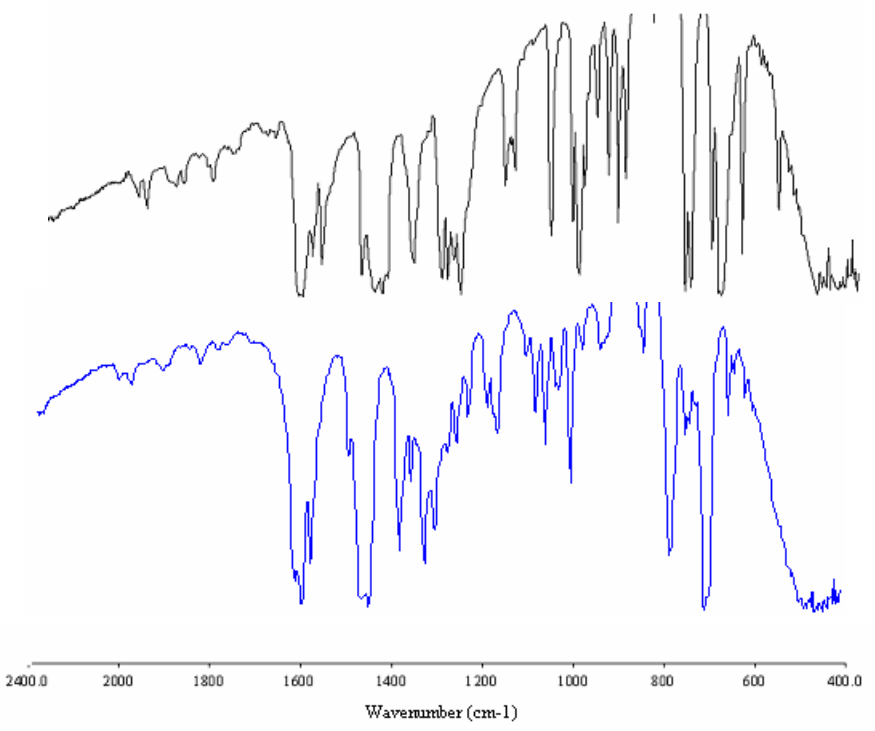

Figure 2.17 IR spectra of ligand **L8** (top) and complex **10** (bottom)

The same shift can be seen when comparing the infrared spectra of complex **11** and ligand **L9**

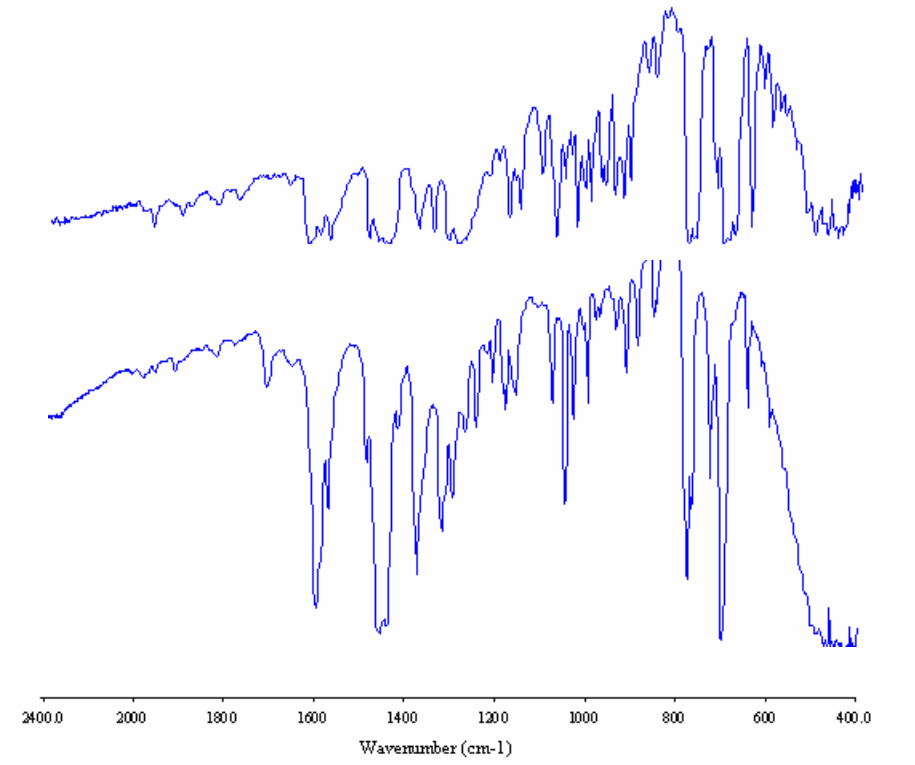

Figure 2.18 IR spectra of ligand **L9** (top) and complex **11** (bottom)

2.4.2.1.3 Characterization by means of Elemental Analysis

Table 2.12 gives the elemental results of complexes **10** and **11**. The calculated and found values for the percentage carbon, hydrogen and nitrogen correspond very well for both complexes. These results therefore support the fact that the desired complexes were obtained.

Table 2.12 Elemental analysis results of complexes **10** and **11**

Complex	Elemental Analysis	
	Calculated	**Found 1**
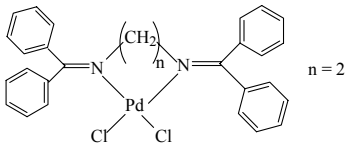 n = 2 *Complex* **10**	**C**: 54.44% **H**: 4.28% **N**: 4.95%	54.84% 3.70% 4.82%
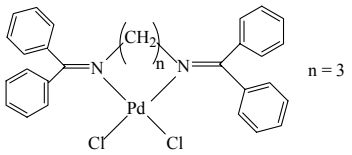 n = 3 *Complex* **11**	**C**: 60.01% **H**: 4.52% **N**: 4.83%	60.11% 4.56% 4.59%

2.5 Conclusion

All ligands were successfully synthesized. By reacting the ligands with either $PdCl_2(COD)$ or $PdCl_2(CH_3CN)_2$ the desired complexes of both α-diimine and unconjugated β-diimine ligands were obtained. However when using $Pd(OAc)_2$ as the palladium source, it was found that the ligands **L6** and **L7** did not coordinate to the metal through both nitrogens of the diimine system but through the nitrogen of the pyridine ring and the oxygen of the carboxyl group.

2.6 Experimental

General Details

All experiments were carried out under an atmosphere of purified nitrogen using standard Schlenk techniques. Diethyl ether and THF were dried by distillation over sodium wire/benzophenone. Acetone was dried by distillation over anhydrous calcium chloride and CH_2Cl_2 dried by distillation over phosphorous pentoxide. Methanol was dried by distilling it over a Grignard complex formed *in situ* by reacting magnesium turnings with iodine. Solvents (AR grade) were obtained from Kimix Chemicals. The dried solvents were stored in Schott bottles over 0.4 nm molecular sieves from Merck. The functionalized amines used as starting materials as well as the pyridine-2-carboxaldehyde were purchased from Sigma-Aldrich and used without further purification. $PdCl_2(COD)$ and $PdCl_2(CH_3CN)_2$ were synthesized according to literature procedures[17]. The $PdCl_2$ used for this as well as the $Pd(OAc)_2$ used in the formation of *Complex* **8** and *Complex* **9** were purchased from Next Chimica (Pty) Ltd (South Africa).

2.6.1 Synthesis of Ligands

Preparation of L1

A slight excess of allylamine (1.87 ml, 25 mmol) was added dropwise to a stirred solution of pyridine-2-carboxaldehyde (1.98 ml, 21 mmol) in dry diethyl ether (10 ml) cooled in an ice bath. After complete addition of the amine, anhydrous $MgSO_4$ (0.50 g) was added and the slurry stirred for 2h at room temperature. The reaction mixture remained an orange colour for the duration of the stirring. The mixture was filtered and the solvent removed from the filtrate to obtain a golden yellow oil. The crude product

was extracted with water. The product was dissolved in hexane to which water was added and the mixture shaken. The organic layer was collected and dried over anhydrous $MgSO_4$. The mixture was filtered and the solvent removed from the filtrate to obtain a yellow oil of mass 2.66 g (86% yield).

Preparation of L2

Pyridine-2-carboxaldehyde (0.81 ml, 9 mmol) was added to 4-vinylaniline (1.0 ml, 9 mmol) in 5.0 ml of dry diethyl ether while stirring. Anhydrous $MgSO_4$ (0.025 g) was added and the slurry stirred for 2h. After this time the mixture was filtered and the solvent removed from the filtrate. The crude product was dissolved in $CHCl_3$. Water was added to this solution and the mixture shaken up. Two layers separated of which the organic layer was collected. Anhydrous $MgSO_4$ was added to this layer. This was filtered and the solvent removed from the filtrate to obtain a golden yellow oil of mass 1.59 g (85% yield).

Preparation of L3[18]

An excess of propylamine (2.01 ml, 25 mmol) was added dropwise to a stirred solution of pyridine-2-carboxaldehyde (1.98 ml, 21 mmol) in diethyl ether (10 ml) cooled in an ice bath. After complete addition of the amine, anhydrous $MgSO_4$ (0.5 g) was added and the slurry stirred at room temperature for 2h. The mixture was filtered and the solvent removed from the filtrate to obtain an orange oil. The oil was dissolved in hexane. Water was added to this solution and the mixture shaken up. Two layers separated of which the organic layer was collected. Anhydrous $MgSO_4$ was added to this layer after which it was

filtered and the filtrate concentrated to dryness. A yellow oil of mass 2.52 g (68% yield) was obtained.

Analytically Calculated for $C_9H_{12}N_2PdCl_2$: C 33.21%, H 3.72%, N 8.61%. Found: C 33.37%, H 3.25%, N 8.18%

Preparation of L4 [18]

1-Pentylamine (3.0 ml, 25 mmol) was added to a stirred solution of dry diethyl ether (10 ml) and pyridine-2-carboxaldehyde (2.0 ml, 21 mmol) cooled in an ice bath. After complete addition of the amine, 0.5 g anhydrous $MgSO_4$ was added to the mixture. This was stirred for 2h at room temperature. After this time the solution was filtered and the solvent removed. A golden yellow oil of mass 2.47 g (66.9% yield) was obtained.

Analytically Calculated for $C_{11}H_{14}N_2PdCl_2$: C 37.37%, H 4.56%, N 7.92%. Found: C 37.14%, H 4.19%, N 7.47%

Preparation of L5

4-Aminophenol (2.73 g, 25 mmol) was dissolved in dry THF (120 ml) and slowly added to pyridine-2-carboxaldehyde (1.98 ml, 21 mmol) dissolved in dry THF (10 ml). Anhydrous $MgSO_4$ (3.0 g) was added to the solution and the mixture stirred for 30min. at room temperature. After this time the mixture was filtered and the solvent removed from the filtrate. A yellow solid of mass 4.09 g was obtained (83% yield).

Preparation of L6

NaOH (0.3 g, 7.44 mmol) was dissolved in 30 ml methanol in a beaker. Aminocaproic acid (1.0 g, 7.6 mmol) was dissolved in the NaOH solution. This solution was filtered and the filtrate concentrated to dryness to obtain a white residue. The white residue was redissolved in methanol (30 ml) and (1.1 ml, 11.5 mmol) pyridine-2-carboxaldehyde slowly added whilst stirring. This solution was stirred at room temperature for 4h. After this time the solvent was removed to obtain an orange oil. Acetone was added to the oil and stirred. This resulted in the oil becoming an off white waxy material. The waxy material was allowed to settle and the supernatant acetone syringed off. Diethyl ether was added to the waxy material and this also stirred up. Again the product was allowed to settle and the supernatant diethyl ether syringed off. This washing procedure was repeated twice more. The waxy product was transferred to a Schlenk tube and dried under vacuum.

Preparation of L7

Preparation is the same as for **L6** but using 4-aminobutyric acid as the starting material.

Preparation of L8 and L9[16]

The ligands were synthesized by refluxing 30mmol of the diamine, benzophenone (10.9 g, 60 mmol) and $CaSO_4$ (9.0 g, 73 mmol) in a 100 ml round bottomed flask using 50 ml anhydrous methanol as solvent. The reaction was monitored by infrared spectroscopy until the product peak (1621 cm^{-1}) was larger than the benzophenone carbonyl peak (1658 cm^{-1}). Once this was observed (2 weeks for the ethanediamine starting material, 4

weeks for the propanediamine starting material and 3 weeks for the butanediamine starting material) the solution was cooled and filtered by suction. The solid was washed with 50 ml methanol. This was air dried and soxhlet extraction from $CaSO_4$ with 150 ml heptane was performed overnight. Upon cooling, crystals of pure product were filtered from heptane and air dried.

2.6.2 Complex Formation

Formation of *Complex* 1

$PdCl_2(CH_3CN)_2$ (0.078 g, 0.3 mmol) was dissolved in dry acetone (10 ml) in an N_2-purged Schlenk tube. Ligand **L1** (0.048 g, 0.3 mmol) was also dissolved in dry acetone (5.0 ml) in an N_2-purged Schlenk tube. The yellow ligand solution was added under a stream of nitrogen to the orange $PdCl_2(CH_3CN)_2$ solution. This resulted in the formation of a yellow precipitate. The mixture was stirred at room temperature for 24h. After this time the precipitate was allowed to settle and the supernatant liquid syringed off. The precipitate was washed with dry acetone (5.0 ml), allowed to settle and the supernatant liquid syringed off again. The remaining solvent was removed on the vacuum line. A yellow solid of mass 0.0608 g (63% yield) was obtained.

Formation of *Complex* 2

$PdCl_2(COD)$ (0.1 g, 0.3 mmol) was dissolved in dry CH_2Cl_2 (10 ml) in an N_2-purged Schlenk tube. Ligand **L2** (0.075 g, 0.3 mmol) was dissolved in dry CH_2Cl_2 (5.0 ml) in an N_2-purged Schlenk tube. The yellow ligand solution was added under a stream of nitrogen to the yellow $PdCl_2(COD)$ solution. This resulted in the formation of a yellow

precipitate. The solution was stirred at room temperature for 24h. After this time the solution was filtered and the residue washed with firstly with a 5.0 ml portion of hexane and with a 5.0 ml portion of CH_2Cl_2 and allowed to dry. The mass of the yellow solid obtained was 0.0718 g (62% yield)

Formation of *Complex* 3

$PdCl_2$(COD) (0.1 g, 0.3 mmol) was dissolved in dry CH_2Cl_2 (10 ml) in an N_2-purged Schlenk tube. Ligand **L3** (0.051 g, 0.3 mmol) was dissolved in dry CH_2Cl_2 (5.0 ml) in an N_2-purged Schlenk tube. The yellow ligand solution was added under a stream of nitrogen to the yellow $PdCl_2$(COD) solution. This resulted in the formation of a yellow precipitate. After stirring the reaction mixture for 24h at room temperature, it was filtered and washed with a 5.0 ml portion of hexane and a 5.0 ml portion of CH_2Cl_2 and allowed to dry. A yellow solid of mass 0.053 g (63% yield) was obtained.

Formation of *Complex* 4

$PdCl_2$(COD) (0.05 g, 0.15 mmol) was dissolved in dry CH_2Cl_2 (10 ml) in an N_2-purged Schlenk tube. Ligand **L4** (0.035 g, 0.15 mmol) was dissolved in dry CH_2Cl_2 (5.0 ml) in an N_2-purged Schlenk tube and added under a stream of nitrogen to the yellow $PdCl_2$(COD) solution. After approximately 35min of stirring at room temperature there was the appearance of pale yellow precipitate. Stirring was continued for 1h after appearance of the precipitate. After this time the mixture was filtered and the residue washed with a 5.0 ml portion of hexane and a 5.0 ml portion of CH_2Cl_2. A light yellow solid of mass 0.013 g (19% yield) was obtained.

Formation of *Complex* 5

$PdCl_2(CH_3CN)_2$ (0.078 g, 0.3 mmol) was dissolved in dry acetone (10 ml) in an N_2-purged Schlenk tube. Ligand **L5** was dissolved in dry acetone (5.0 ml) in an N_2-purged Schlenk tube and added under a stream of nitrogen to the orange $PdCl_2(CH_3CN)_2$ solution. This resulted in a clear orange solution that was stirred for 24h at room temperature. After this time the solvent was removed under vacuum to yield an orange solid (82% yield).

Formation of *Complex* 6

$PdCl_2(CH_3CN)_2$ (0.078 g, 0.3 mmol) was dissolved in dry acetone (10 ml) in an N_2-purged Schlenk tube. Ligand **L6** (0.080 g, 03 mmol) was dissolved in dry MeOH (5.0 ml) in an N_2-purged Schlenk tube and added under a stream of nitrogen to the orange $PdCl_2(CH_3CN)_2$ solution. This resulted in the immediate appearance of a light brown precipitate. The mixture was stirred at room temperature for 15min. After this time the precipitate was allowed to settle and the supernatant liquid syringed off. The remaining light brown solid was washed with a mixture of 5.0 ml dry acetone and 5.0 ml dry MeOH. The solid was allowed to settle and the supernatant liquid syringed off. The washing process was repeated. The product was dried under vacuum to yield a pale yellow solid (72% yield).

Formation of *Complex* 7

The same procedure as for *Complex* **6** was followed, but in this case using ligand **L7**. A pale yellow solid was obtained (65% yield).

Formation of *Complex* 8

$Pd(OAc)_2$ (0.0673 g, 0.3 mmol) was dissolved in dry CH_2Cl_2 (5.0 ml) in an N_2-purged Schlenk tube. Ligand **L6** (0.0600 g, 0.24 mmol) was stirred up in dry CH_2Cl_2 (5.0 ml) in an N_2-purged Schlenk tube to form a brown suspension of the ligand in the solvent. This was added under a stream of nitrogen to the orange $Pd(OAc)_2$ solution. This resulted in the immediate formation of a pale yellow precipitate. The mixture was stirred at room temperature for 15mins. After this time the solid was allowed to settle and the supernatant liquid syringed off. The remaining yellow solid was washed with dry CH_2Cl_2 (5.0 ml) to remove any unreacted $Pd(OAc)_2$. The washing procedure was repeated and the solid dried on the vacuum line (58% yield).

Formation of *Complex* 9

The same procedure as for *Complex* **8** was followed, but in this case using ligand **L7** (52% yield).

Formation of *Complexes* 10 and 11

$PdCl_2(CH_3CN)_2$ (0.0780 g, 0.3 mmol) was dissolved in dry acetone (5.0 ml) in an N_2-purged Schlenk tube. The desired ligand (**L8** or **L9**) (0.3 mmol) was also dissolved in dry acetone (5.0 ml) in an N_2-purged Schlenk tube. The clear ligand solution was added under a stream of nitrogen to the orange $PdCl_2(CH_3CN)_2$ solution. This caused a lightening of the orange colour with a yellow precipitate forming soon after that. In total the mixture was stirred for 15 minutes at room temperature. After this time the precipitate was allowed to settle and the supernatant liquid syringed off. The residue was washed

with 10ml dry acetone. The product was again allowed to settle and the supernatant liquid syringed off. The product was dried under vacuum. Both complexes **10** and **11** were isolated as yellow solids with an approximate yield of 77%.

2.7 References

1. Ittel, S.D., Johnson, L.K., Brookhart, M., *Chem. Rev.*, **2000**, *100*, 1169.
2. Johnson, L.K., Killian, C.M., Brookhart, M., *J. Am. Chem. Soc.*, **1995**, 23, 6414.
3. Johnson, L.K., Mecking, S., Brookhart, M., *J. Am. Chem. Soc.*, **1996**, *118*, 267.
4. Van Koten, G., Vrieze, K., *Adv. Organomet. Chem.*, **1982**, *21*, 532.
5. Meneghetti, S.P., Lutz, P.J., Kress, J., *Organometallics*, **1999**, *18*, 2734.
6. Köppl, A., Alt, H.G., *J. Mol. Cat. A: Chem*, **2000**, *154*, 45.
7. Laine, T.V., Piironen, U., Lappalainen, K., Klinga, M., Aitola, E., Leskelä, M., *J. Organomet. Chem.*, **2000**, *606*, 112.
8. Chen, R, Bacsa, J, Mapolie, S.F., *Polyhedron*, **2003**, *22*, 2855.
9. Parks, J.E., Holm, R.H., *Inorg. Chem.*, **1968**, *7*, 1408.
10. Landolsi, K., Rzaigui, M., Bouachir, F., *Tetrahedron Letters*, **2002**, *43*, 9463.
11. Honeybourne, C.L., Webb, G.A., *Chem. Commun.*, **1968**, 739.
12. Feldman, J., McLain, S.J., Parthasarathy, A., Marschall, W.J., Calabrese, J.C., Arthur, S.D., *Organometallics*, **1997**, *16*, 1514.
13. Clegg, W., Cope, E.K., Edwards, A.J., Mair, F.S., *Inorg. Chem.*, **1998**, *37*, 2317.
14. Cope-Eatough, E.K., Mair, F.S., Pritchard, R.G., Warren, J.E., Woods, R.J., *Polyhedron,* **2003**, *22*, 1447.

15. Nakamoto, K. (1969). *Infrared Spectra of Inorganic and Coordination Compounds (Second Edition)*. New York: Wiley-Intersience.

16. Datta, D., *J. Chem, Soc., Dalton Trans*, **2000**, 235.

17. Anderson, G.K., Lin, M., *Inorg. Synth.*, **1990**, *28*, 60.

18. Haddleton, D.M., Crossman, D.C., Dana, D.H., Duncalf, D.J., Heming, A.M., Kukulj, D., Shooter, A.J., *Macromolecules*, **1999**, *32*, 2110.

Chapter 3

Catalytic Evaluation of Functionalized Pyridinyl Diimine Complexes of Palladium

3.1 Introduction

3.1.1 α-Diimine Complexes as Catalyst Precursors for Olefin Polymerization

Brookhart discovered that Pd(II) and Ni(II) diimine catalyst systems of the type $\{[ArN=C(R)-(R)C=NAr]M(CH_3)(OEt_2)\}^+BAr'_4^-$ (Ar = 2,6-$(Me)_2C_6H_3$, 2,6-(i-Pr)$_2C_6H_3$), were capable of polymerizing ethylene and α-olefins to high molecular weight polymers with controlled level of polymer branching[1]. The key feature of these catalysts is that the axial coordination sites are blocked by the presence of bulky *ortho* aryl substituents at the imino nitrogen. This thus retards the rate of chain termination resulting in high molecular weight polymers.

Other research groups have studied asymmetrical bidentate aryl substituted pyridylimine-type catalysts and found that Ni(II) catalysts yielded only oligomers whereas Pd(II) analogues were found to be inactive[2-4]. However Chen and coworkers reported on pyridylimine-type Pd(II) complexes with long straight alkyl groups attached to the imino nitrogen that yielded highly linear polyethylene with high molecular weights[5].

Chen *et al* found that the complex bearing the longest alkyl chain showed the lowest activity as compared to the other complexes in their study, but produced polymers with the highest molecular weight (M_w = 22 x 10^5). They thus showed that by changing the substituents on the imino nitrogen from an aryl group to a long chain alkyl group has the effect of greatly increasing molecular weights and producing linear polyethylene.

Various techniques are used to characterize polymers. Differential Scanning Calorimetry (DSC) gives an idea of whether the polymer is linear or not. The temperature at which the polymer melts (T_m) indicates this. When T_m is in the range 135-137°C it indicates that the polymer is linear polyethylene. Further evidence for linear polyethylene can be obtained by looking at the high temperature ^{13}C $\{^1H\}$ NMR spectrum of the polymer. If a single peak is observed it indicates no branching has occurred thus resulting in linear high density polyethylene.

Gel Permeation Chromatography (GPC) gives the number average molecular weight (M_n) and the weight average molecular weight (M_w). The polydispersity index (PDI) is the ratio that represents the extent of molecular weight distribution. It is the ratio of the number average molecular weight (M_n) to the weight average molecular weight (M_w).

In this chapter complexes similar to that of Chen and coworkers are evaluated in their catalytic activity towards ethylene polymerization. The difference is that there is now a functionality attached at the end of the alkyl chain. The activity and type of polymer produced by the functionalized pyridinyl diimine complexes is then compared to those complexes prepared by Chen and coworkers.

The activity towards ethylene polymerization of the unconjugated β-diimine complexes prepared in Chapter 2 is also investigated and compared to that of conventional β-diimine complexes as well as that of the functionalized pyridinyl diimine complexes.

3.1.2 Heck Coupling Reactions

The palladium-catalyzed reaction in which the carbon group of a haloalkene or haloarene is substituted for a vinylic hydrogen is known as a Heck reaction[6]. Equation 3.1 illustrates this. It is particularly valuable in synthetic organic chemistry because it is the only general method yet discovered for this type of substitution.

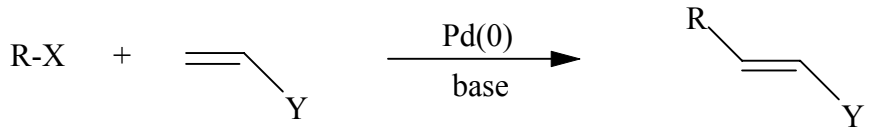

(3.1)

The most common halides used are aryl, heterocyclic, benzyl and vinylic iodides and bromides, with iodides being generally more reactive. A wide range of functionalized groups, including alcohols, ethers, aldehydes, ketones and esters may be present elsewhere in the organohalide or alkene without reacting themselves or affecting the Heck reaction. The reactivity of the alkene is a function of steric crowding about the C=C bond. The greater the degree of substitution on the double bond the slower the reaction and the lower the yield.

Commonly used bases are tertiary amines such as triethylamine, or sodium or potassium acetate and sodium hydrogen carbonate with the reaction taking place in polar aprotic solvents such DMF, CH_3CN or DMSO.

The form of the palladium catalyst most commonly added to the reaction medium is $Pd(OAc)_2$. The catalytically active Pd(0) form of the metal is generated *in situ* by

reduction of the Pd(II). The catalyst, $Pd(0)L_2$, is formed by reaction with added PPh_3. $PdCl_2L_2$ [L = PPh_3 or P(*o*-tolyl)$_3$] is often also used as precatalyst. The catalyst then reacts with the organohalide to begin the catalytic cycle as shown in Scheme 3.1. The main role of the tertiary monophosphine ligands is to stabilize the zerovalent palladium preventing the formation of inactive palladium black.

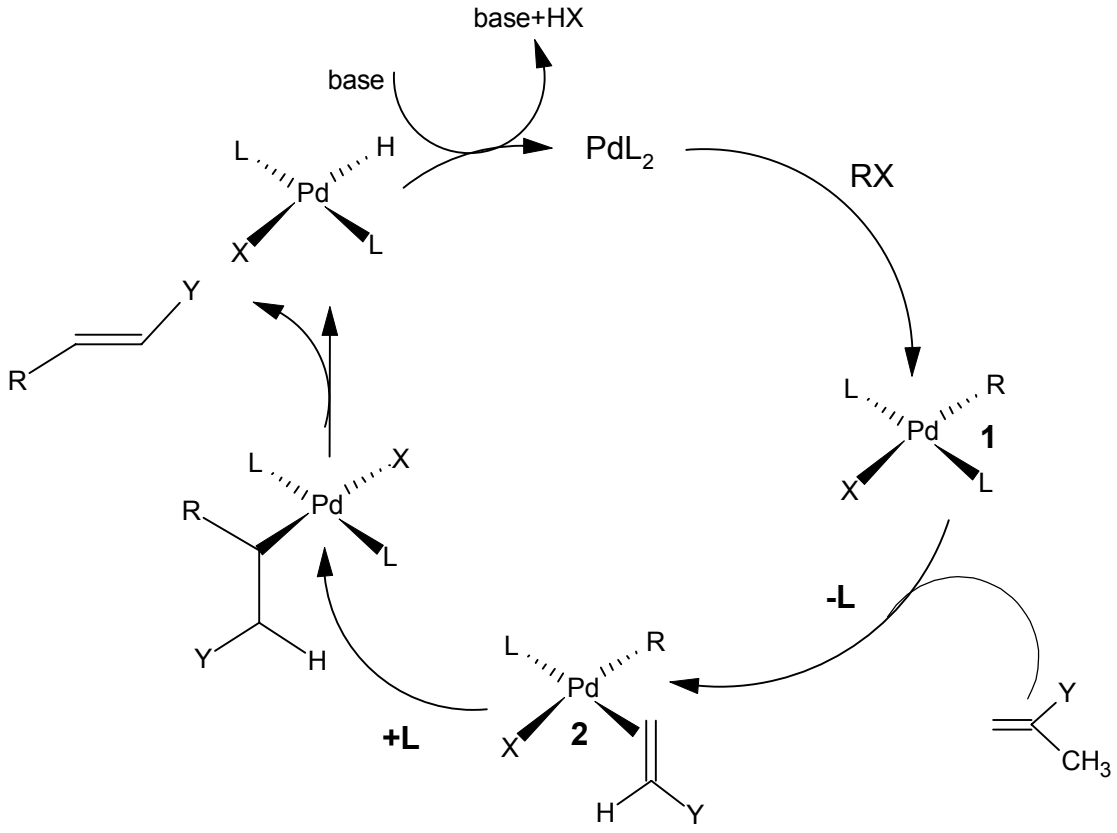

Scheme 3.1 Mechanism for Heck coupling reaction[7]

The catalytically active coordinatively unsaturated Pd(0) species complex is independent of the source of the palladium. This is because the species is electron rich and nucleophilic in character and has vacant sites so that the organohalide can undergo

oxidative addition to give the known $RPdXL_2$ intermediate (**1**) in which the aryl or vinyl R group is σ-bonded to the Pd(II). The intermediate (**1**) is the *trans* isomer, which is formed by an isomerization of the thermodynamically less stable *cis* isomer. A vacant site is then created to accommodate and activate the alkene. This happens when the monodentate phosphine ligand dissociates so that a neutral $RPdXL(CH_2=CH-Y)$ (**2**) species is formed.

Scheme 3.2 shows how the coordinated alkene then undergoes *syn* addition to form an unstable σ-bonded complex, which will rotate around the C-C bond so that the palladium and β-hydrogen are *syn* co-planar and β-hydride elimination takes place to generate the observed *trans* substituted alkene and the catalytically inactive $HPdXL_2$.

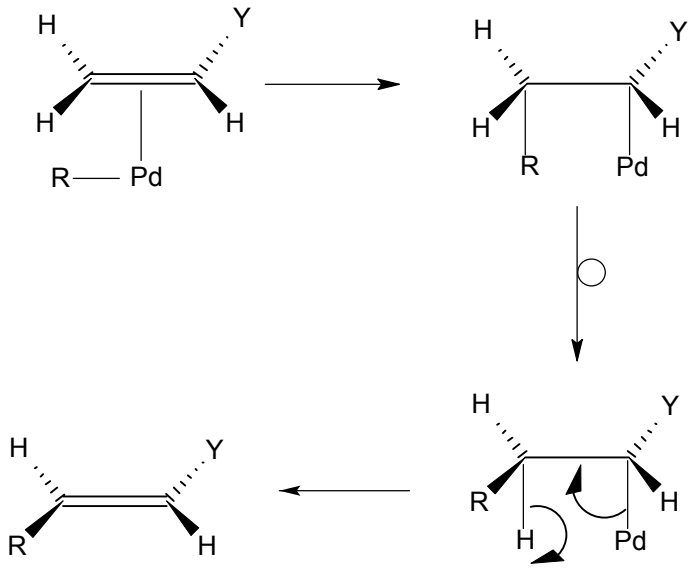

Scheme 3.2 Generation of observed *trans* substituted alkene

The presence of a base in the cycle is important since it facilitates reductive elimination of HX from $HPdXL_2$ to regenerate the Pd(0) species. The cycle is then repeated.

It has been shown that the use of electron rich, sterically bulky tertiary phosphines can be employed as catalyst modifiers in Heck coupling reactions[8-11]. The ligand properties in these cases make it possible for less reactive aryl bromides and chlorides to be utilized in Heck reactions.

The monophosphine palladium complexes are in many cases air-sensitive. The P-C bond is also subject to degradation at the temperatures commonly employed under Heck conditions (usually around 80°C). To counteract this, higher phosphine concentrations are needed which would however lead to elevated costs especially in large-scale applications. In this regard nucleophilic *N*-heterocyclic carbenes, the imidizole-2-ylidenes, have attracted extensive attention since they show considerable stabilizing effects in organometallic systems with respect to heat, moisture and air while having similar electronic and steric properties as compared to basic phosphines[12, 13].

Other catalytic systems evaluated in the Heck reaction are Pd(II) cyclometallated imine systems. These systems however require high reaction temperatures and long reaction times[14, 15].

Systems containing the 1,4-diaza-1,3-butadiene skeleton (DAB-R) have also been evaluated by Grasa and coworkers[16]. Figure 3.1 shows the general structure of the DAB-R ligands used.

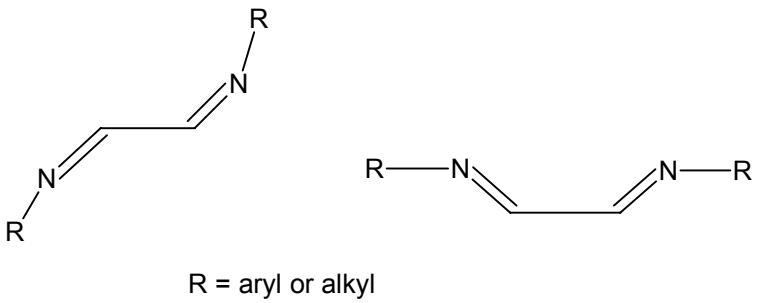

Figure 3.1 Diazabutadiene (DAB-R) ligands

These α-diimine ligands were of interest because of their σ-donating and low π-accepting abilities as well as their relative cost-effectiveness in preparation. Pd(II)-α-diimine complexes were synthesized from $Pd(OAc)_2$ and the catalytic activity of these systems tested in the Heck reaction. Figure 3.2 gives an example of the type of complexes formed and evaluated for their catalytic activity.

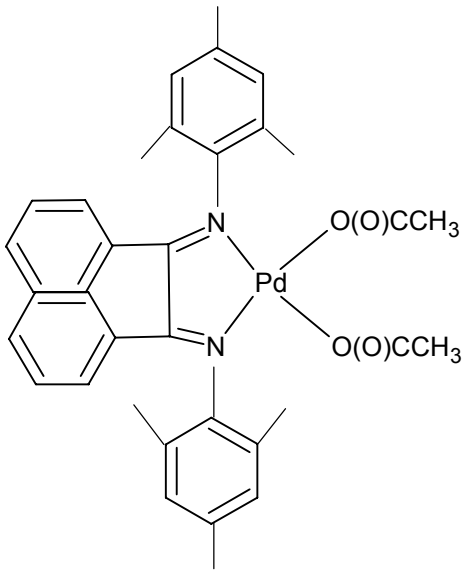

Figure 3.2 Example of complex whose catalytic activity was evaluated in Heck reactions by Grasa *et al*.

It was reported that these types of complexes show high activity with respect to coupling of electron-neutral and electron-deficient aryl bromides with a variety of olefins. Particularly high activity and selectivity were observed for styrenes. Square planar Pd(II)(DAB-R)$(OAc)_2$ complexes were also found to be excellent precatalysts for Pd(0)$(DAB\text{-}R)^-$ ionic species generated in the polar solvent *N,N*-dimethylacetamide (DMAc).

In this chapter the catalytic activity towards Heck coupling reactions of the functionalized pyridinyl diimine complexes that were synthesized in Chapter 2 is also evaluated. The activity of the unconjugated diimine ligands are also looked at and compared to that of the functionalized α-diimine complexes.

3.2 Evaluation of Catalytic Activity of Complexes

3.2.1 Evaluation of Catalytic Activity of Functionalized α-Diimine Complexes of Palladium towards Ethylene Polymerization

The palladium complexes were activated in toluene by the addition of a 10% w/w toluene solution of methylaluminoxane (MAO) at room temperature in a glovebox. This was done utilizing varying Al:Pd ratios so as to find the optimum ratio which produces the best turn over number for each catalyst precursor. Ethylene polymerization was carried out at 5 atm of ethylene pressure in an autoclave. All the polymeric products were white granular solids. The products were characterized by DSC, high temperature ^{13}C $\{^{1}H\}$ NMR spectroscopy and GPC.

The only functionalized α-diimine complexes showing any activity towards ethylene polymerization were complexes **1**, **2** and **5** (Figure 3.3). The results are shown in Table 3.1. The activity of complex **3** which bears no functionality was also evaluated for the sake of comparison.

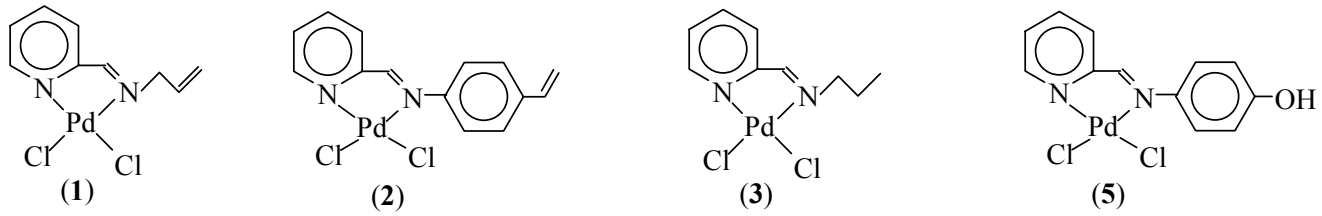

Figure 3.3 Complexes showing activity towards ethylene polymerization

Table 3.1 Results of ethylene polymerization catalyzed by complexes **1**, **2**, **3** and **5**

Catalysts	Al/Pd	Activity kg PE (mol Pd atm h)$^{-1}$	M_n[a] x 10^{-5}	M_w[a] x 10^{-5}	PDI[b]
1	250	0	-	-	-
1	500	74.0	3.99	10.3	2.59
1	1000	67.6	4.29	11.7	2.72
1	1500	36.2	6.28	15.1	2.40
1	2000	0	-	-	-
3	250	0	-	-	-
3	500	58.3	2.24	6.54	2.24
3	1000	46.3	2.46	6.05	2.47
3	1500	27.1	2.63	6.26	2.38
3	2000	0	-	-	-
2	500	1.50	5.94	14.7	2.47
2	1000	5.60	6.90	17.6	2.55
2	1500	14.0	5.65	12.9	2.29
2	2000	0	-	-	-
5	500	0	-	-	-
5	1000	8.17	4.14	12.6	3.05
5	2000	133.8	3.42	8.97	2.63
5	3000	12.8	4.58	12.0	2.63
5	3500	0	-	-	-

Polymerization conditions: [Pd] = 0.015mmol, 100ml toluene, 5 atm, 1h, 25°C
[a] Molecular weight data determined by GPC vs. polyethylene standards at 160°C
[b] PDI = M_w/M_n

Activity was observed at the Al/Pd ratios as indicated in Table 3.1. Complex **5** exhibited optimum activity of 133 kg PE/mol Pd atm h at a Al/Pd ratio of 2000:1 whereas the optimum activity of complex **2** of 14.0 kg PE/mol Pd atm h was reached at a Al/Pd ratio of 1500:1. This indicates that varying electronic properties of similar aromatic ligands has an effect on the activity of complexes towards ethylene polymerization; the ligand bearing the more electronegative functionality being almost ten times more active at a

slightly higher Al/Pd ratio. The need for the higher Al/Pd ratio when utilizing complex **5** is possibly due to the presence of the OH group. This OH group most likely first reacts with MAO which means that an excess of MAO is then required to obtain the active catalytic species. The formation of Al alkoxides are known[17]. Comparing the activity of complexes **1** and **3**, it can be seen that the functionalized diimine ligand complex is slightly more active than the complex having the same carbon chain length but bearing no functionality.

GPC analysis showed that these functionalized pyridinyl imine palladium complexes produced high molecular weight polyethylene (M_n = 4.0-7.0 x 10^5, M_w = 11-17 x 10^5). The PDI values were found to be fairly similar for each complex, ranging between 2.50 and 3.00. These values are typical of high density polyethylene[5]. By comparing the molecular weights of the polymers produced by complexes **2** and **5**, it can be seen that complex **2** produces slightly higher molecular weight polymers as compared to complex **5**. It can thus be seen that the more electronegative functionality, although increasing activity, slightly inhibits chain growth resulting in the slightly lower molecular weight polymers.

On the other hand, comparing the molecular weights of the polymers produced by complexes **1** and **3**, it can be seen that complex **1**, bearing the allyl functionality, produces higher molecular weight polymers. The functionality thus seems to increase both activity and the molecular weight of the polymers produced.

DSC (T_m = 135-137°C) showed that all the polymeric material had melting points similar to high-density linear polyethylene. Figure 3.4 shows the DSC trace that is typical of the type of polymer produced.

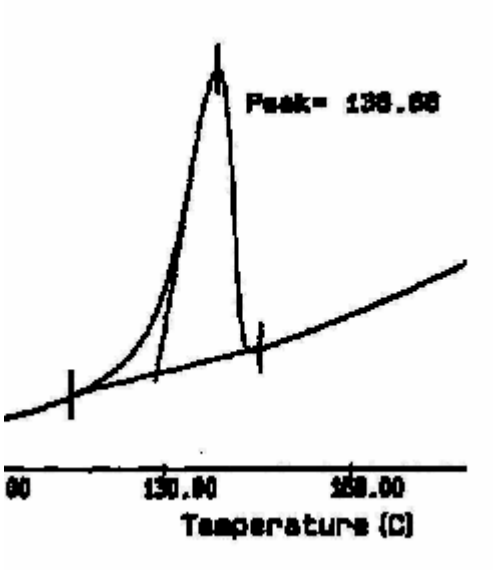

Figure 3.4 DSC trace typical of polymer produced

The appearance of only one signal in the high temperature ^{13}C $\{^1H\}$ NMR spectra of the polymerization products confirms their linear nature. Figure 3.5 is a ^{13}C $\{^1H\}$ NMR spectrum that is characteristic of the polymer produced.

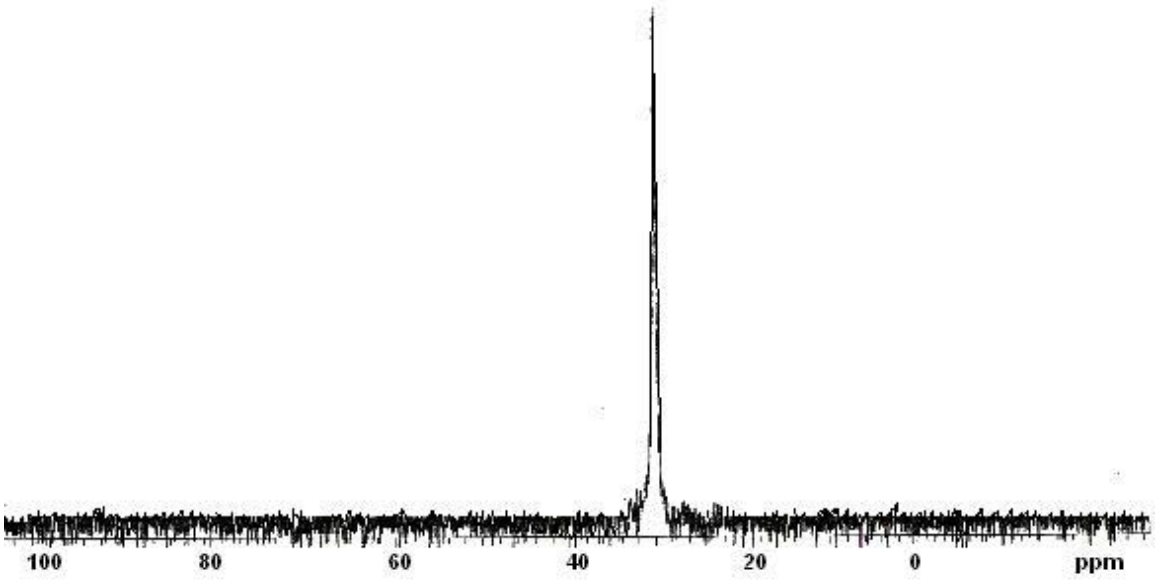

Figure 3.5 High temperature $^{13}C\{^{1}H\}$NMR spectrum which is typical of the polyethylene produced.

The molecular weights of the polymer produced as well as the PDI values are similar to the results obtained by Chen and coworkers in their investigation into the catalytic activity towards ethylene polymerization of their pyridylimine Pd(II) complexes with long straight alkyl chains attached to the imino nitrogen[5]. The activity of complex **2** was found to be comparable to those of Chen *et al* at similar Al:Pd ratios (in the range 500:1 to 2000:1).

The ω-carboxylato ligand complexes in which $PdCl_2(CH_3CN)_2$ was used as palladium source (complexes **6** and **7**, Figure 3.6), showed no activity towards ethylene polymerization even at high Al/Pd ratios of up to 6000:1. This is probably due to these ionic precursors being insoluble in the non-polar polymerization medium (toluene).

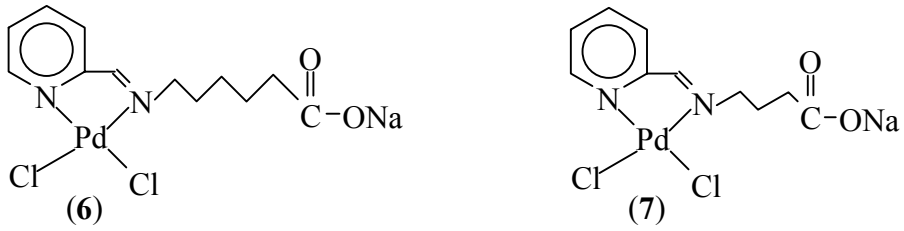

Figure 3.6 ω-carboxylato ligand complexes in which $PdCl_2(CH_3CN)_2$ was used as palladium source

3.2.2 Evaluation of Catalytic Activity of β-Diimine Complexes of Palladium towards Ethylene Polymerization

The unconjugated β-diimine ligand complexes (complexes **10** and **11**, Figure 3.7) were also evaluated but found to be inactive towards ethylene polymerization at Al:Pd ratios of 500:1, 1000:1, 2000:1 and 3000:1. The inactivity could be due to the steric bulkiness of the phenyl groups hindering the MAO from abstracting the chlorine molecule necessary for activation of the complex.

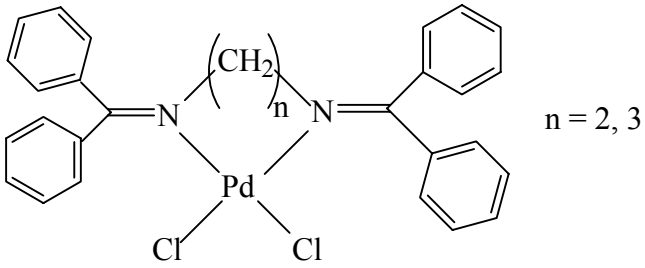

Figure 3.7 Unconjugated β-diimine ligand complexes **10** (n = 2) and **11** (n = 3)

3.2.3 Evaluation of Catalytic Activity of Functionalized α-Diimine Complexes of Palladium towards Heck Coupling Reactions

The catalytic activity of complexes **1**, **2** and **5**-**7** were tested towards the Heck coupling of iodobenzene with methyl acrylate (Equation 3.2). Reactions were carried out under an

atmosphere of purified nitrogen at 80°C using dry CH_3CN as solvent in the presence of triethylamine as base for 8h. Equivalent molar ratios of iodobenzene, methyl acrylate and triethylamine were used. The catalyst precursor was added at a 1:100 Pd:substrate molar ratio. A sample of the reaction mixture without any of the catalyst precursor present was first withdrawn. This was to determine (by means of Gas Chromatography-Mass Spectroscopy) the initial amount of iodobenzene present before commencement of the arylation reaction. After addition of the catalyst precursor, samples were withdrawn at periodic intervals and the consumption of iodobenzene monitored by GC-MS.

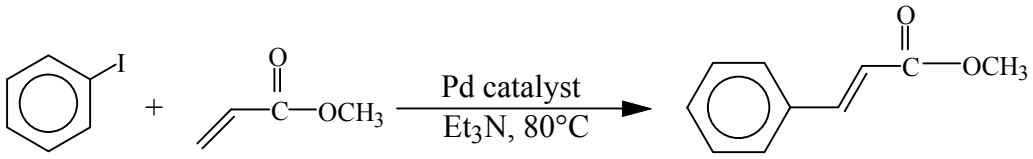

(3.2)

With each catalyst precursor evaluated the major product formed by the Heck coupling reaction was the *trans* stereoisomer, methyl (2*E*)-3-phenylacrylate. The *cis* stereoisomer, methyl (2*Z*)-3-phenylacrylate, observed comprised less than 1% of the isomeric products formed.

Figure 3.8 gives the percentage conversion of iodobenzene versus time using complexes **1** and **2** as catalyst precursors. Their activity is compared to that of $PdCl_2$ in the absence of any ligand.

It can thus be seen that complexes **1** and **2** are more active than the uncoordinated $PdCl_2$ in the arylation reaction of methyl acrylate, yielding an almost 80% conversion of the

iodobenzene after only one hour. Complex **1** was however found to be slighty less active than complex **2** (60% iodobenzene conversion after one hour), but reached the approximately the same percentage of iodobenzene conversion after eight hours.

A similar evaluation of complexes **5**-**7** as catalyst for Heck coupling was conducted. Figure 3.9 gives the percentage conversion of iodobenzene versus time using complexes **5**, **6** and **7** as catalyst precursors. Their activities are also compared to that of $PdCl_2$. It can thus be seen from this that complexes **5**, **6** and **7** show similar trends in activity in the arylation reaction, all of them achieving about a 70% conversion of iodobenzene after one hour and resulting in a 90% conversion after eight hours while being more active than the uncoordinated $PdCl_2$.

The activity of these catalyst precursors are slightly higher compared to the diazabutadiene complexes utilized in the Heck coupling reaction of 1-bromo-4-methylbenzene with methyl acrylate by Grasa *et al* using a DAB-Cy catalyst precursor at a higher temperature of 100°C (Equation 3.3).

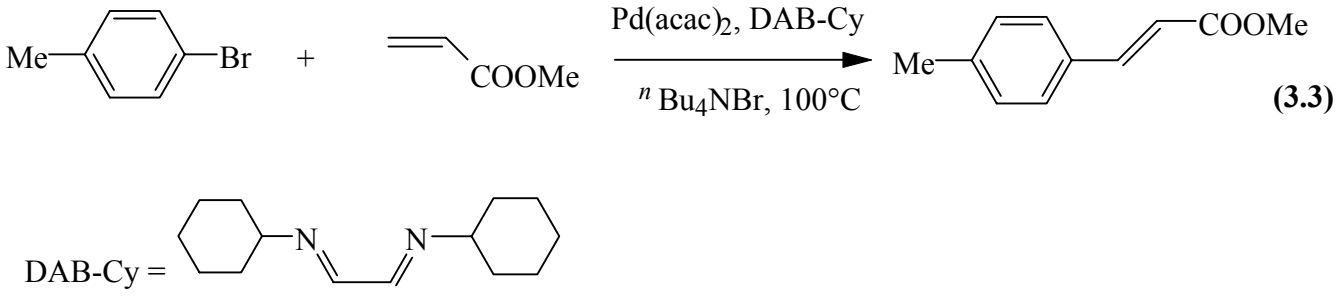

(3.3)

A 58% conversion was achieved after six hours with the DAB-Cy catalyst precursor as compared to the 80% conversion achieved with the α-diimine ligand complexes.

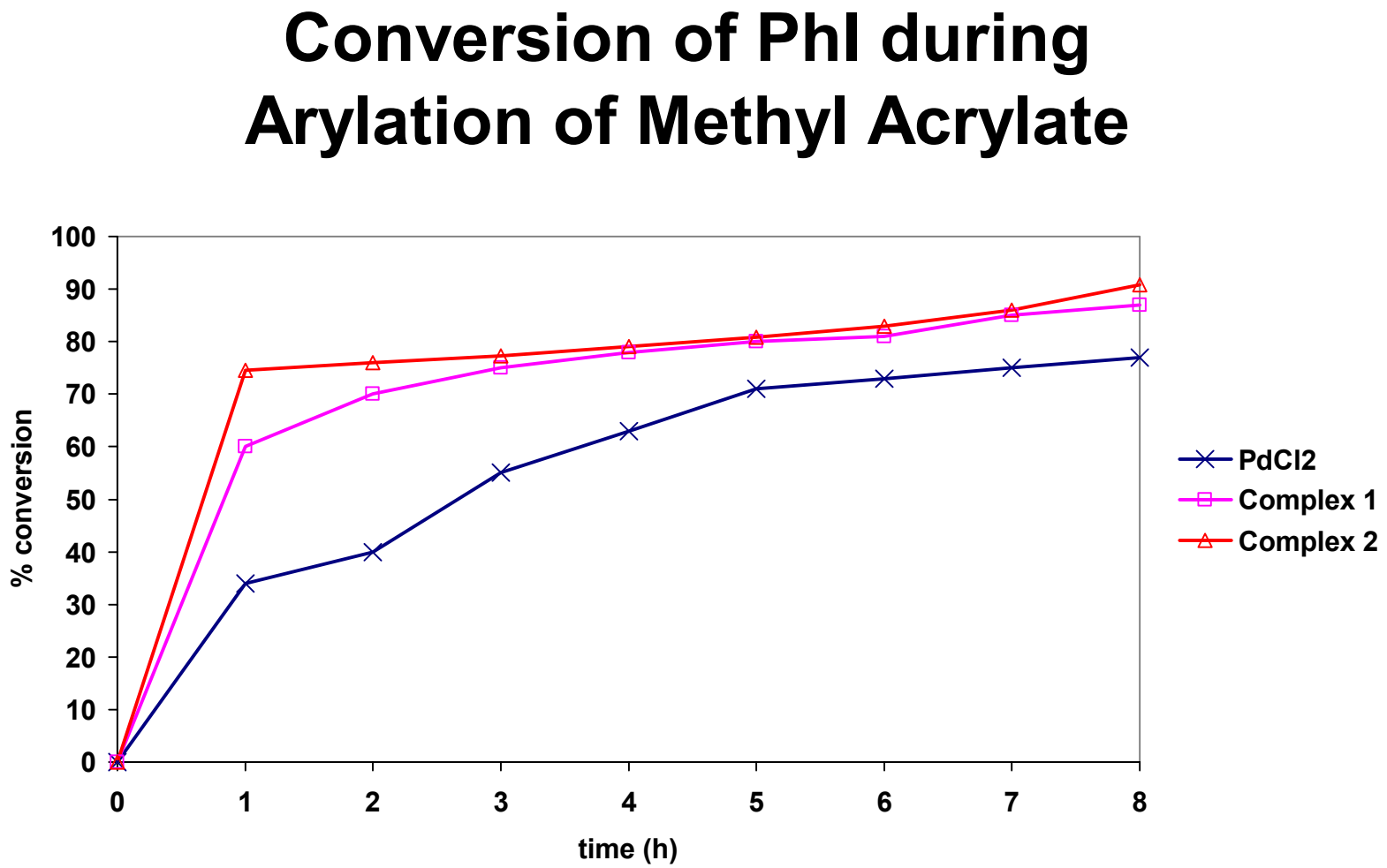

Figure 3.8 Conversion of iodobenzene *vs.* time plot for the arylation of methyl acrylate using $PdCl_2$, Complex **1** and Complex **2** as precatalysts

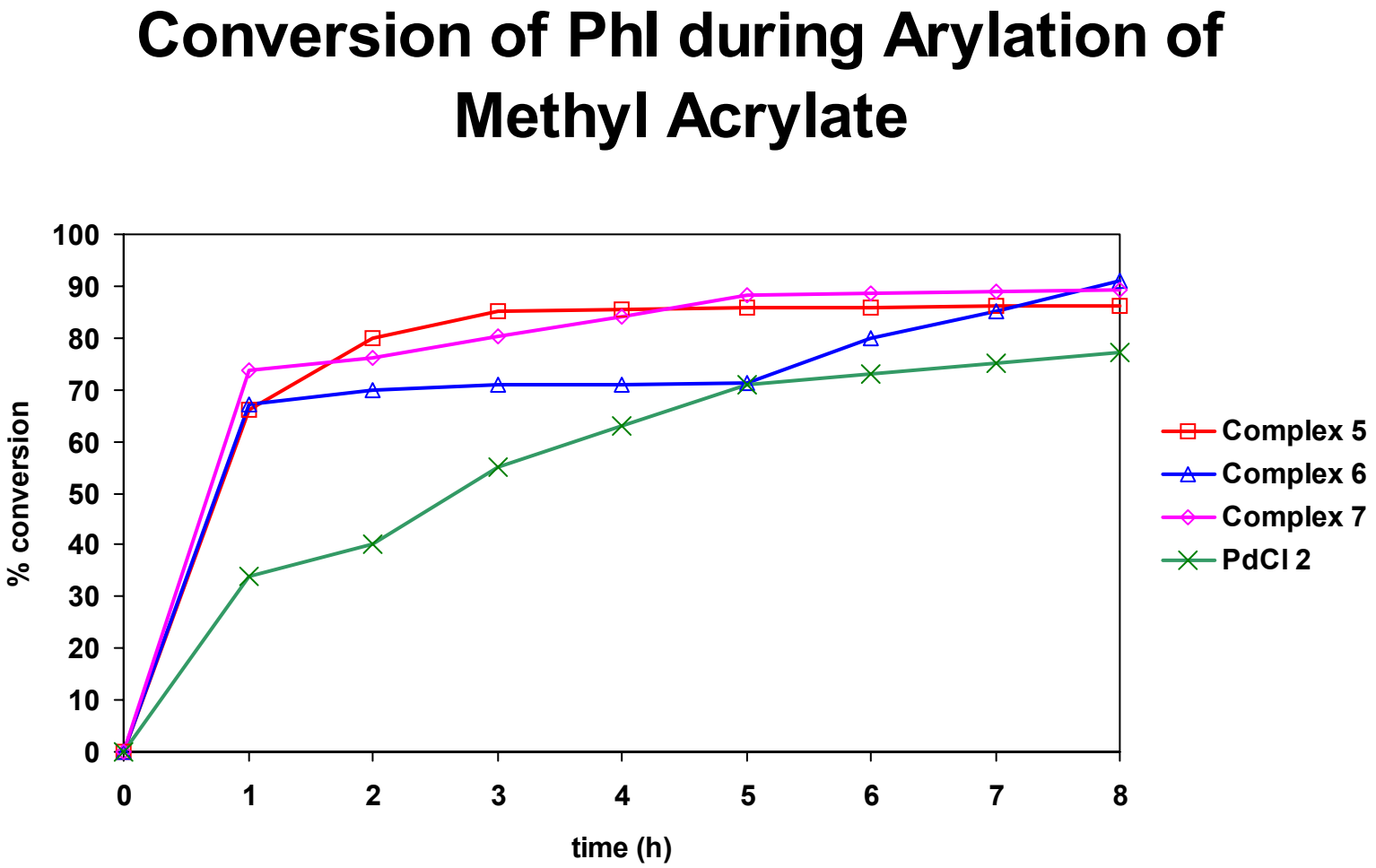

Figure 3.9 Conversion of iodobenzene *vs*. time plot for the arylation of methyl acrylate using complexes **5**, **6**, **7** and $PdCl_2$ as catalyst precursors

3.2.4 Evaluation of Catalytic Activity of Unconjugated β-Diimine Ligand Complexes of Palladium towards Heck Coupling Reactions

The same reaction conditions were employed as when evaluating the functionalized α-diimine ligand complexes as catalyst precursors. Figure 3.10 shows the percentage conversion of iodobenzene versus time when using complexes **10** and **11** as catalyst precursors and again comparing it to the activity of the uncoordinated $PdCl_2$. It can be seen from Figure 3.10 that these complexes show almost identical activity to the functionalized α-diimine complexes. The activity of these complexes could have been expected to be less due to the steric hindrance that would have been imparted by the four phenyl rings of the ligand towards the reaction of the aryl halide (iodonenzene) with the catalyst which starts the catalytic cycle. The different steric and electronic properties of the unconjugated β-diimine complexes therefore do not show any advantage or disadvantage as compared with the α-diimine complexes.

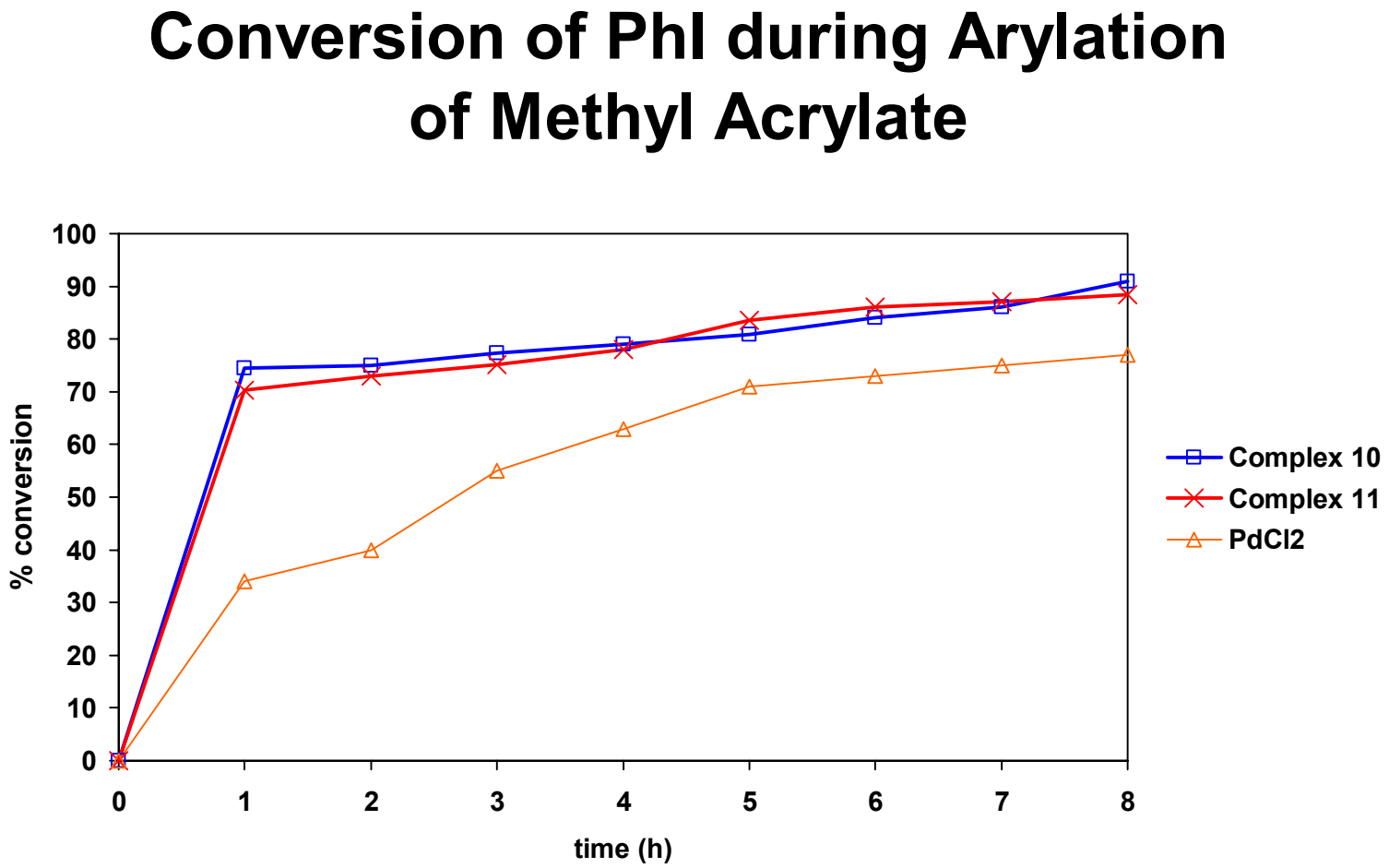

Figure 3.10 Conversion of iodobenzene *vs*. time plot for the arylation of methyl acrylate using complexes **10** and **11** as catalyst precursors

3.3 Conclusion

Only the functionalized α-diimine complexes **1**, **2** and **5** were shown to be catalytically active towards ethylene polymerization. Linear high density polyethylene with high molecular weight was produced. The activity of complexes **1** and **5** were found to be higher than that of the catalysts prepared by Chen and coworkers while that of complex **2** was found to be similar. The unconjugated β-diimine ligand complexes were found to show no activity towards the polymerization of ethylene.

All the functionalized α-diimine complexes were seen to be quite active and exhibit more or less identical activities towards the Heck coupling reaction of iodobenzene with methyl acrylate. Complex **1** was however found to show slightly lower activity which is possibly due the complex acting as both catalyst precursor and competing with methyl acrylate as substrate. This probably happens in complex **1** more easily than with complex **2** because of the closer proximity of the vinyl group to the metal which makes it a more electrophilic olefinic species than compared to complex **2** enabling it to compete with the methyl acrylate as the substrate in the arylation reaction.

These results obtained utilizing the functionalized α-diimine complexes compare favourably with those obtained by Grasa *et al* using α-diimine DAB-R complexes of palladium.

The unconjugated β-diimine ligand complexes showed approximately the same activity towards the Heck coupling of iodobenzene with methyl acrylate as the functionalized α-diimine complexes.

3.4 Experimental

3.4.1. Ethylene Polymerization

The palladium complexes were activated in dry toluene by the addition of a toluene solution of MAO (10% w/w) at room temperature in a glovebox. Polymerization experiments were carried out at 5 atm of ethylene pressure at 25°C for 1h in a 300ml Parr stainless steel autoclave. After 1h the polymerization reaction was quenched by the addition of absolute ethanol (50ml). The reaction mixture was filtered and the obtained polymer placed in a 1M ethanolic HCl solution for a few days. After this time the polymer was collected by means of filtration and dried in an oven at moderate temperature (~40°C) for a few days.

3.4.2 Heck Reactions

Iodobenzene (1.7ml, 15mmol) and methyl acrylate (1.4ml, 15mmol) were syringed into a two-necked round-bottomed flask. Triethylamine (2.1ml, 15mmol) was added as a base and the mixture dissolved in 15ml dry CH_3CN. Before addition of the catalyst, a 250μL sample was withdrawn to determine the initial mass of iodobenzene present by means of GC-MS. The palladium catalyst was then added (0.15mmol) and the mixture refluxed under an atmosphere of nitrogen for 8h. Samples (250μL) were withdrawn at periodic intervals and the consumption of iodobenzene monitored by GC-MS.

3.5 References

1. Johnson, L.K., Killian, C.M, Brookhart, M., *J. Am. Chem. Soc.*, **1995**, *117*, 6414.
2. Meneghetti, S.P., Lutz, P.J., Kress, J., *Organometallics*, **1999**, *18*, 2734.
3. Köppl, A., Alt, H.G., *J. Mol. Cat. A: Chem.*, **2000**, *154*, 45.
4. Laine, T.V., Piironen, U., Lappalainen, K., Klinga, M., Aitola, E., Leskelä, M., *J. Organomet. Chem.*, **2000**, *606*, 112.
5. Chen, R., Bacsa, J., Mapolie, S.F., *Polyhedron*, **2003**, *22*, 2855.
6. Dieck, H.A., Heck, R.F., *J. Org. Chem.*, **1972**, *37*, 2320.
7. Crisp, G.T., *Chem. Soc. Rev.*, **1998**, *27*, 427.
8. Littke, A.F., Fu, G.C., *J. Org. Chem.*, **1999**, *64*, 10.
9. Littke, A.F., Fu, G.C., *J. Am. Chem. Soc.*, **2001**, *123*, 6989.
10. Shaughnessy, K.H., Kim, P., Hartwig, J.F., *J. Am. Chem. Soc.*, **1999**, *121*, 2123.
11. Ehrentraut, A., Zapf, A., Beller, M., *Synlett*, **2000**, *11*, 1589.
12. Regitz, M., *Angew. Chem. Int. Ed.*, **1996**, *35*, 725.
13. Huang, J., Stevens, E.D., Nolan, S.P., Peterson, J.L., *J. Am. Chem. Soc.*, **1999**, *121*, 2674.
14. Weissman, H., Milstein, D., *Chem. Commun.*, **1999**, 1901.
15. Ohff, M., Ohff, A., Milstein, D., *Chem. Commun.*, **1999**, 357.
16. Grasa, G.A., Singh, R., Stevens, E.D., Nolan, S.P., *J. Organomet. Chem.*, **2003**, 1.
17. Xue, W.M., Kung, M.C., Kozlov, A.I., Popp, K.E., Kung, H.H., *Catalysis Today*, **2003**, *85*, 219.

? Library

Signature Not Verified

Digitally signed by Library
DN: cn=Library, o=UWC, ou=LICT, c=ZA
Date: 2005.07.27 13:55:21 Z
Reason: Document is released